12/
2-14-95 JSO

UCRL-ID-119561

# JARLSBERG

## Containment Data Report

Billy Hudson
Ted Stubbs
Ray Heinle

December 1994

Lawrence Livermore National Laboratory

This is an informal report intended primarily for internal or limited external distribution. The opinions and conclusions stated are those of the author and may or may not be those of the Laboratory.
This work was performed under the auspices of the U.S. Department of Energy by Lawrence Livermore National Laboratory under contract No. W-7405-Eng-48.

| Classification Guide | Topic Number | Subject |
|---|---|---|
| COK-88-024 | 1.5.6 | Event announcement |
| NV-89-18 | | Event announcement |
| TCG-WT-1 | 1113 | Contractor identification |
| TCG-WT-1 | 1121 | Personnel identification |
| TCG-WT-1 | 1210 | Geology |
| TVG-WT-1 | 1260 | Crater (map) |
| TCG-WT-1 | 1413 | Statement concerning venting |
| TCG-WT-1 | 1452 | Event announcement |
| TCG-WT-1 | 1831 | Depth of burial |
| TCG-WT-1 | 1843 | Stemming material, amount,etc |
| TCG-WT-1 | 1925 | Diagnostic canister dimensions |
| TCG-WT-1 | 3542.3 | Ground motion |
| TCG-WT-1 | 4810 | Radiation measurement |
| TCG-WT-1 | 4820 | Acceleration, pressure, temperature measurement |

JARLSBERG Instrumentation Summary

| Instrumentation | Fielded | Data Return | Present in this Report |
|---|---|---|---|
| Plug Emplacement[a] | yes | yes | yes |
| Radiation | yes | yes | yes |
| Pressure | | | |
| Stemming | yes | yes | yes |
| Challenge | no | - | - |
| Cavity | no | - | - |
| Atmospheric | no | - | - |
| Motion | | | |
| Free field | yes | yes | yes |
| Surface | yes | yes | yes |
| Plug | yes | yes | yes |
| Stemming | no | - | - |
| Surface casing | yes[a] | yes | yes |
| Emplacement pipe | yes[a] | yes | yes |
| Recording trailer | no | - | - |
| Hydroyield | no | - | - |
| Collapse [b] | yes | yes | yes |
| Stress | yes | yes | yes |
| Strain[c] | yes | yes | yes |
| Other Measurements [d] | yes | no | - |

(a) Relative displacement between stemming, emplacement pipe, and casing.
(b) CLIPER in emplacement hole.
(c) Emplacement pipe, emplacement plug, and stemming.
(d) D–cable indicator for plug emplacement.

Event Personnel

| Containment Physics | | Instrumentation | |
|---|---|---|---|
| B. Hudson | LLNL | C. Cordill | LLNL |
| C. Sisemore | LLNL | T. Valk | LLNL |
| V. Wheeler | LLNL | T. Brown | EG&G/AVO |
| J. Kalinowski | EG&G/AVO | W. Webb | EG&G/NVO |
| T. Stubbs | EG&G/AVO | P. Tanner | EG&G/NVO |

## Table of Contents

## 1. Event Description

### 1.1 Containment summary

JARLSBERG was detonated on August 27, 1983 at 07:00 PDT. All phenomena appeared normal with chimney collapse reaching the ground surface about 15 minutes later. The average radius of the resulting crater was 41.4 m and the depth at surface-ground-zero (SGZ) was 7.0 m.

No radiation was detected above ground and the containment was satisfactory.

### 1.2 Site

JARLSBERG was located in hole U10ca of the Nevada Test Site as shown in Figure 1.1. A depth of burst of 200 m placed the detonation in the layered tuffs about 100 m above the Paleozoic contact and nearly 300 m above the static water level. Geologic cross sections through this hole and plan maps of the local region are shown in Figures 1.2 and 1.3[1]. The stemming plan of the 2.24 m diameter hole is shown in Figure 1.4.

### 1.3 Instrumentation

Containment instrumentation for the emplacement hole is shown in Figure 1.5. Further details of the instrumentation installation is given in Reference 2.

The satellite hole, Ue10aa, was instrumented for both stress and motion as shown in Figure 1.6. The gauge stations were emplaced on a fiber-glass pipe and the 0.31 m diameter hole grouted to within 36 m of the surface with the remainder of the hole stemmed with two-part-epoxy (TPE).

As indicated in Figure 1.7, an array of six vertical motion stations were placed near the ground surface at a depth of 0.61 m.

A pre-shot lightning strike on the grounding system destroyed several transducers and possibly damaged others. Those transducer channels which appeared to have been damaged due to lightning or other phenomena are:

*Emplacement hole:* All strain gauge channels except 82 and all pressure and radiation channels.

*Satellite hole:* Stations 42 and 43, were dead pre-shot; channels 41uv, 47at, 48uv, and 49ut were damaged by shock. Data from all stress (soil pressure) channels except 54s appeared invalid.

*Surface array:* Channels 63av, 64uv, 65uv, and 66uv, were all damaged by EMP.

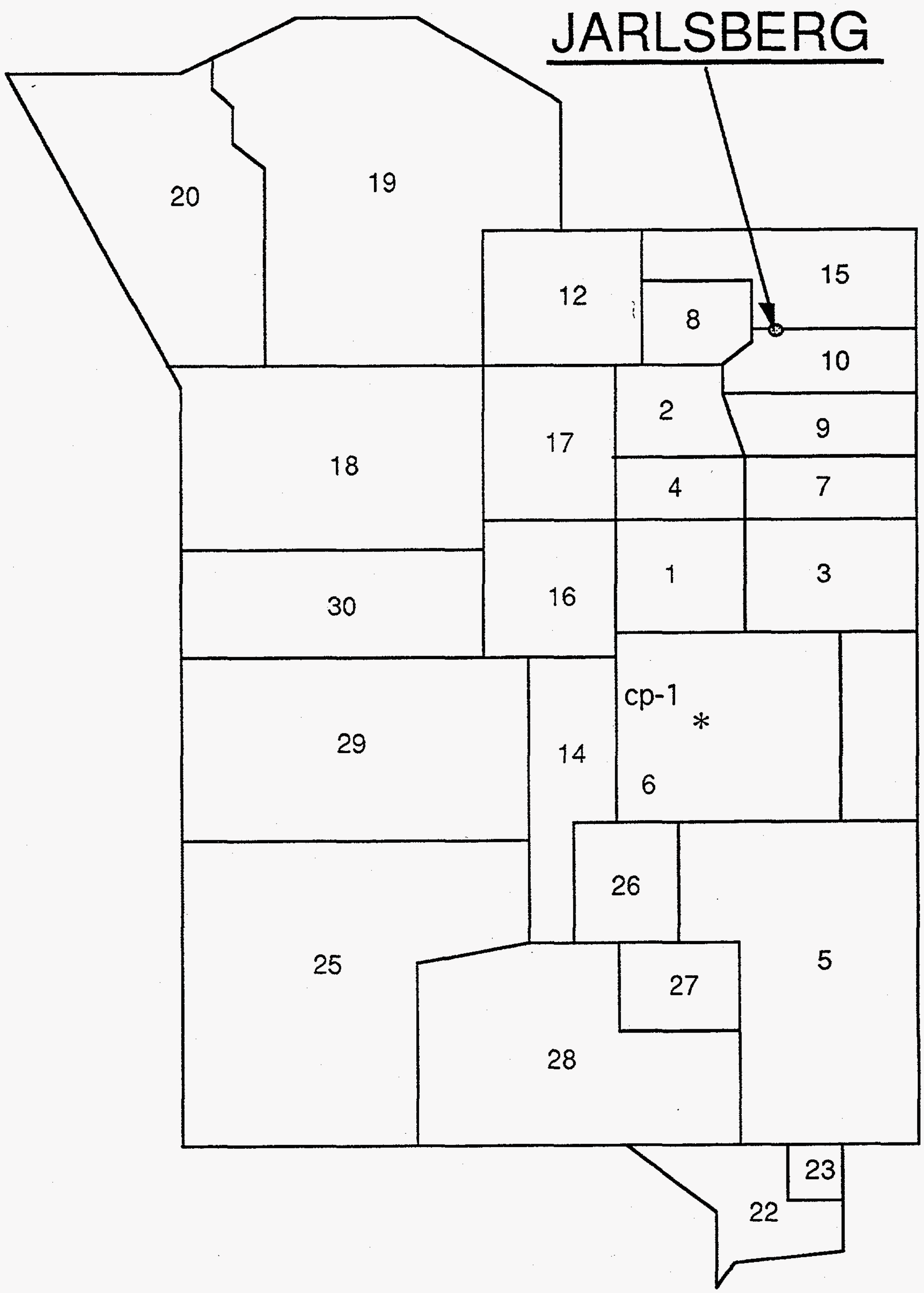


Figure 1.1 Map of the Nevada Test Site indicating the location of hole U10ca.

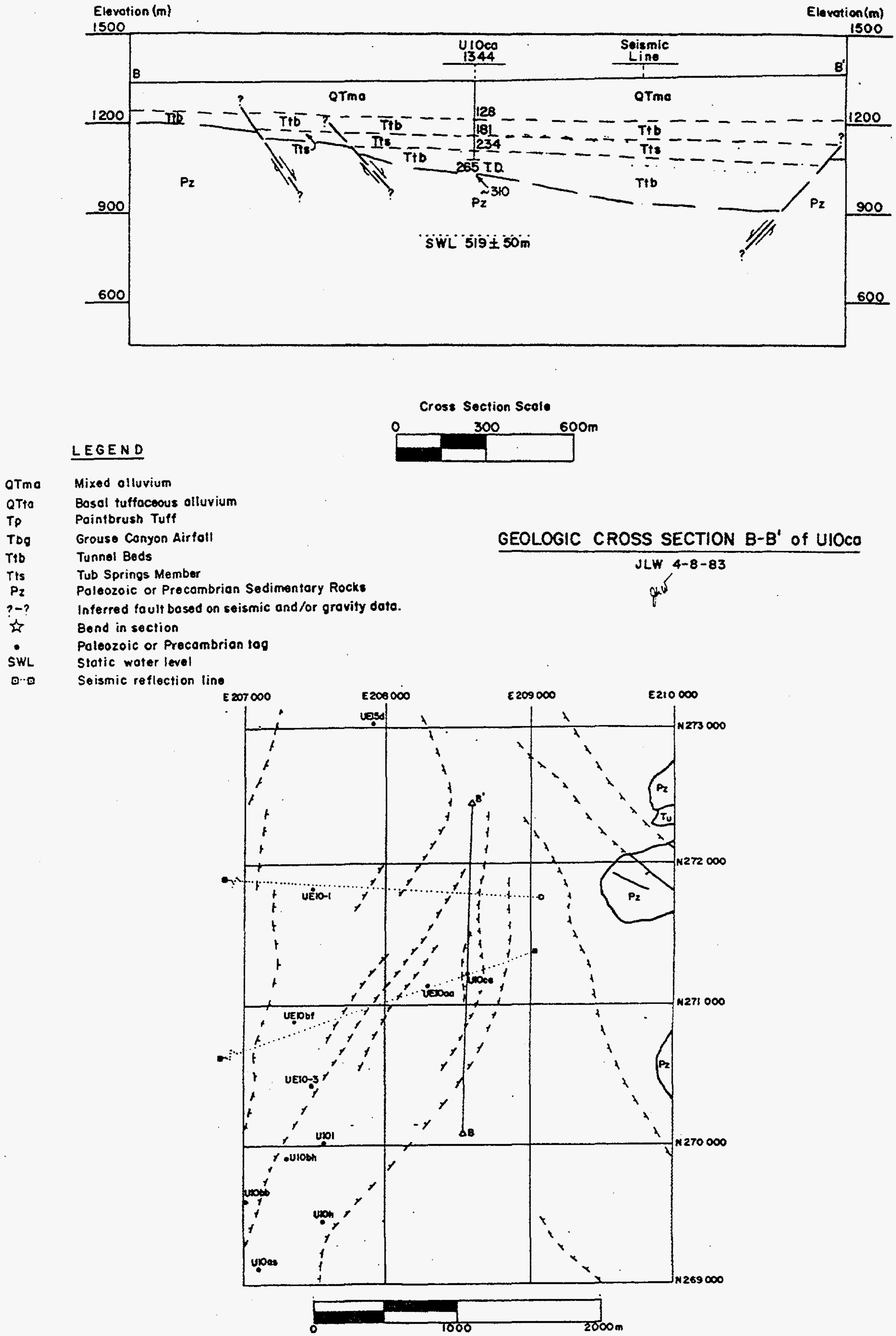


Figure 1.2 Plan view of the region near Hole U10ca with a North–South geologic cross section through the hole.

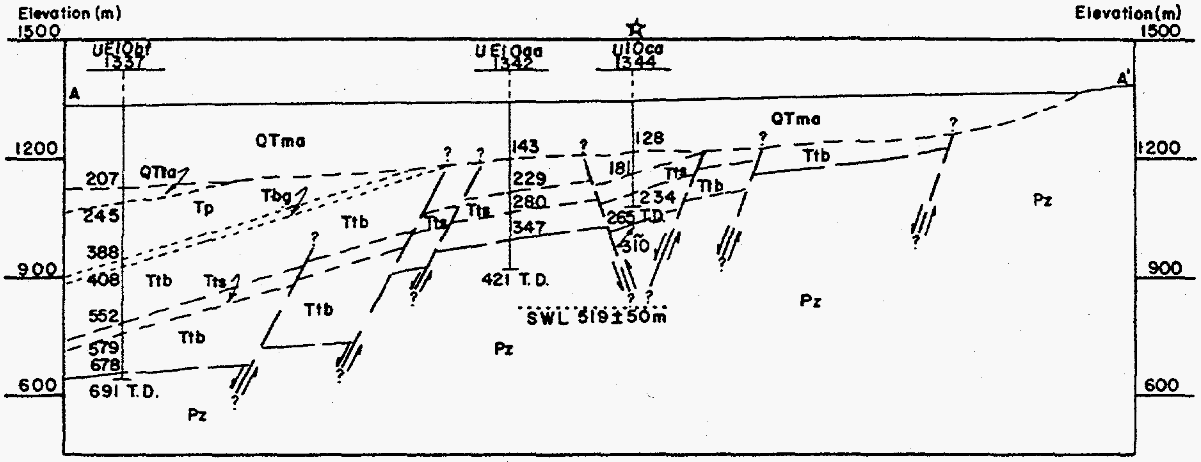


Cross Section Scale
0 300 600m

GEOLOGIC CROSS SECTION A-A' of U10ca

JLW 4-8-83

LEGEND

| | |
|---|---|
| QTma | Mixed alluvium |
| QTta | Basal tuffaceous alluvium |
| Tp | Paintbrush Tuff |
| Tbg | Grouse Canyon Airfall |
| Ttb | Tunnel Beds |
| Tts | Tub Springs Member |
| Pz | Paleozoic or Precambrian Sedimentary Rocks |
| ?–? | Inferred fault based on seismic and/or gravity data. |
| ☆ | Bend in section |
| • | Paleozoic or Precambrian tag |
| SWL | Static water level |
| ⊡-⊡ | Seismic reflection line |

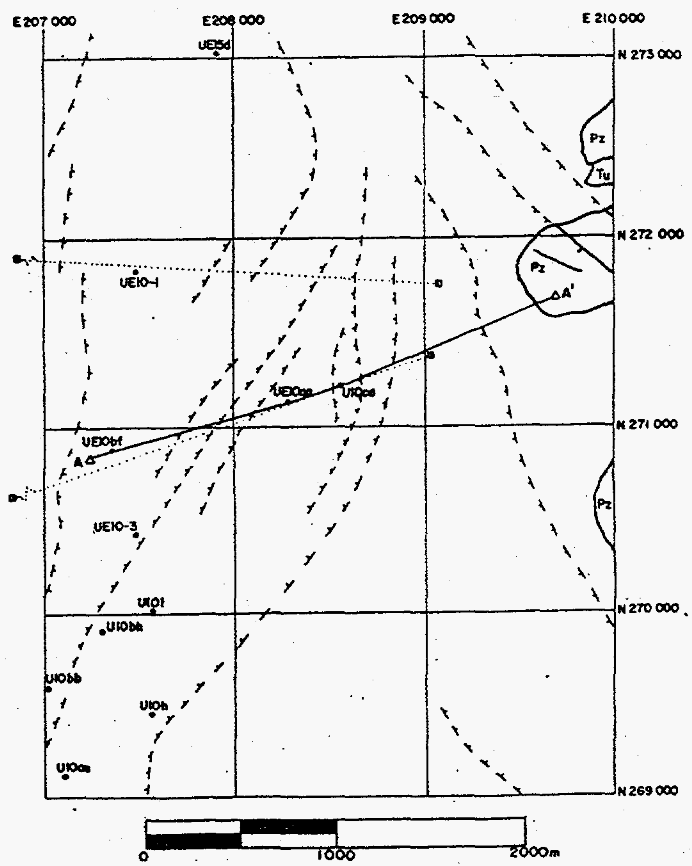


Figure 1.3 Plan view of the region near Hole U10ca with an East–West geologic cross section through the hole.

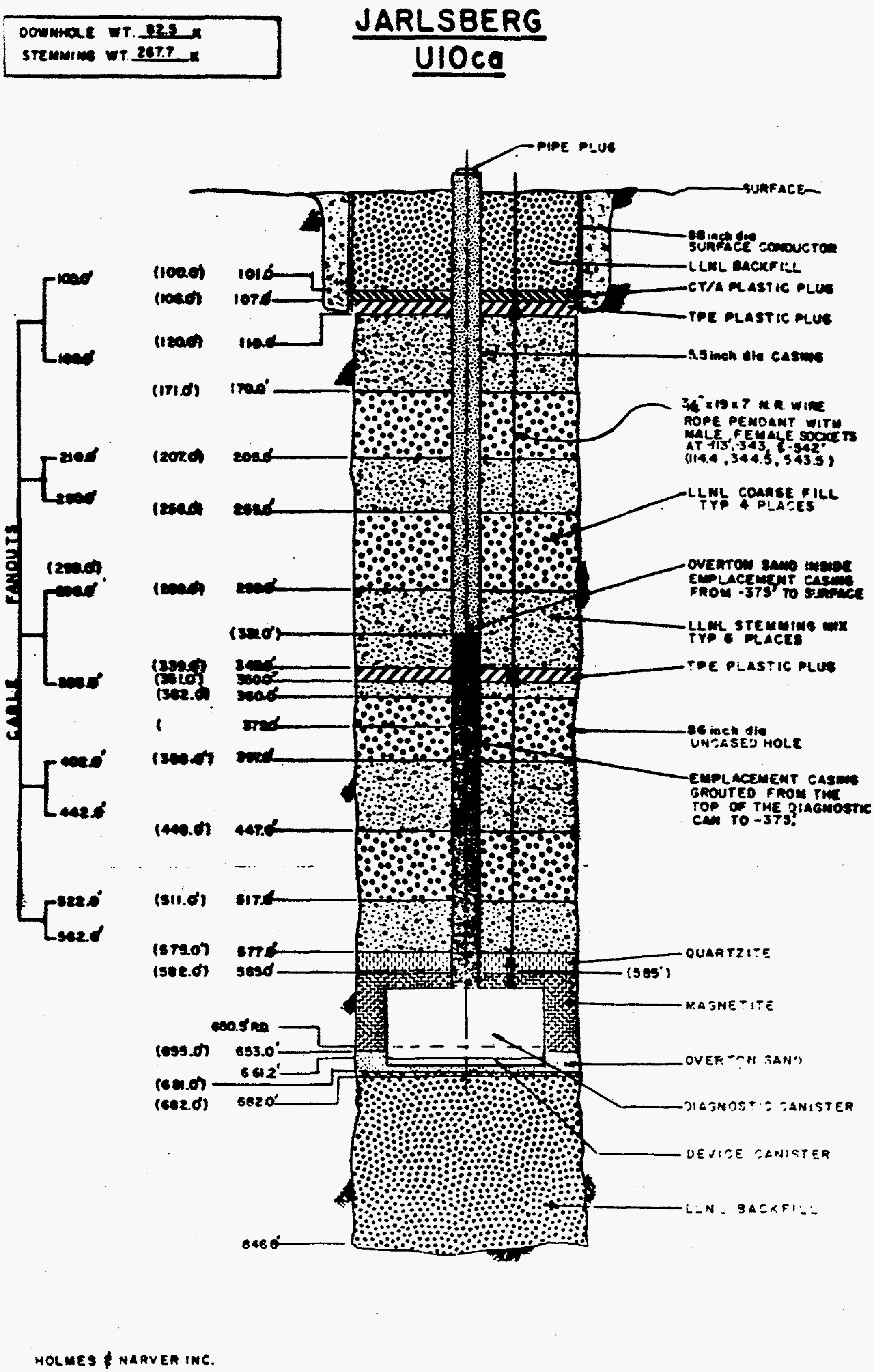


Figure 1.4 As-built stemming plan for hole U10ca.

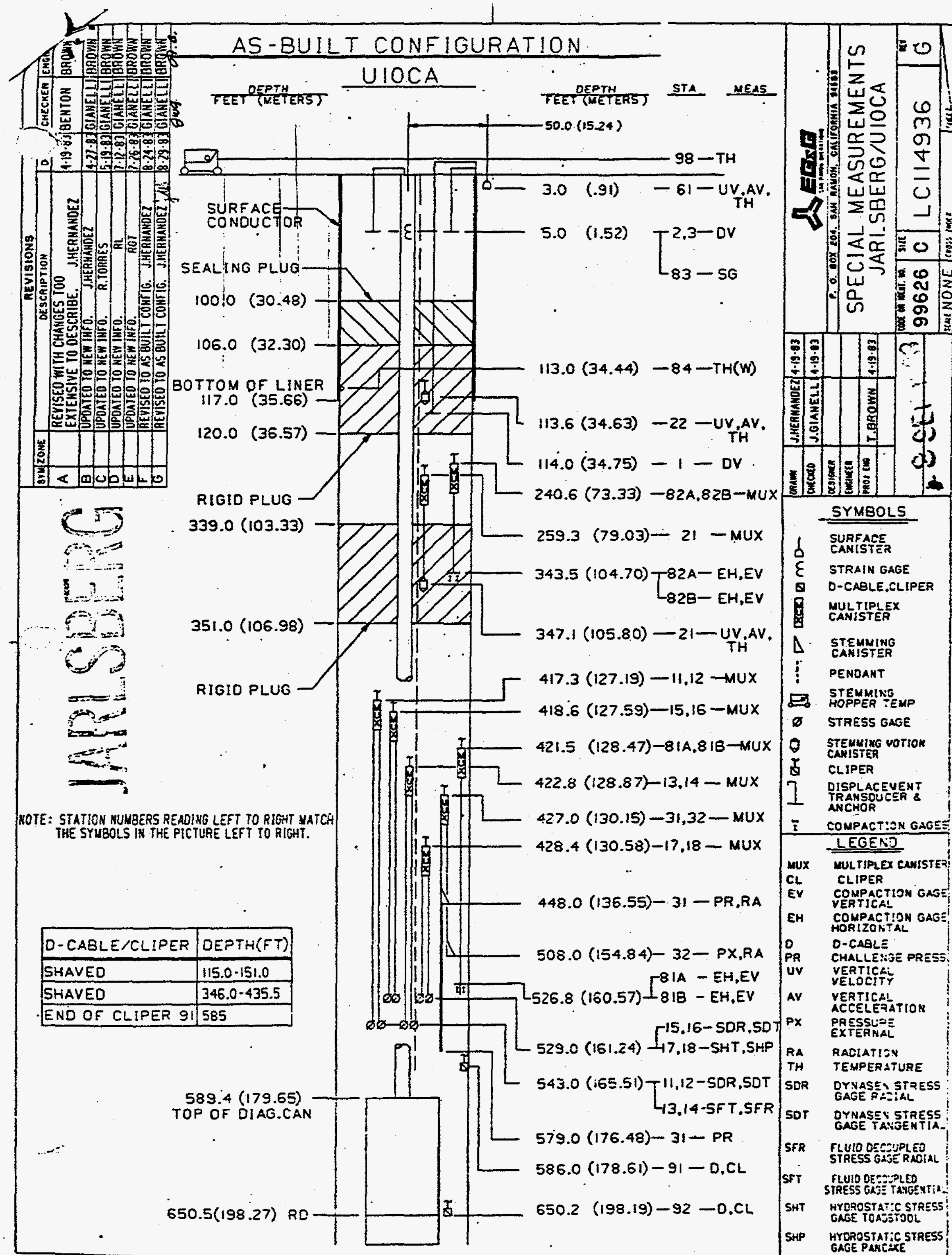


Figure 1.5 As-built instrumentation plan for the JARLSBERG event emplacement hole, U10ca.

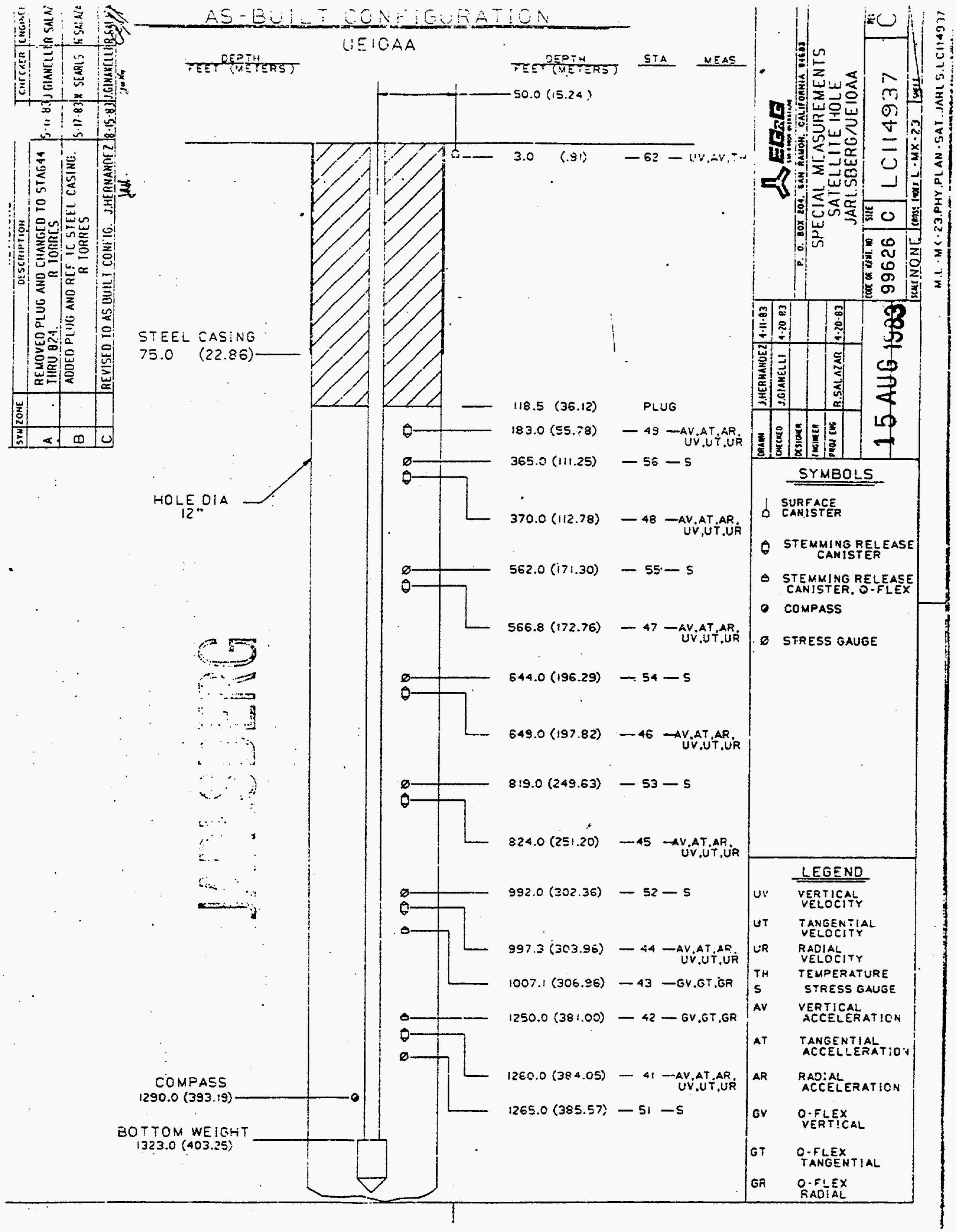


Figure 1.6 As-built instrumentation plan for the satellite hole (Ue10aa).

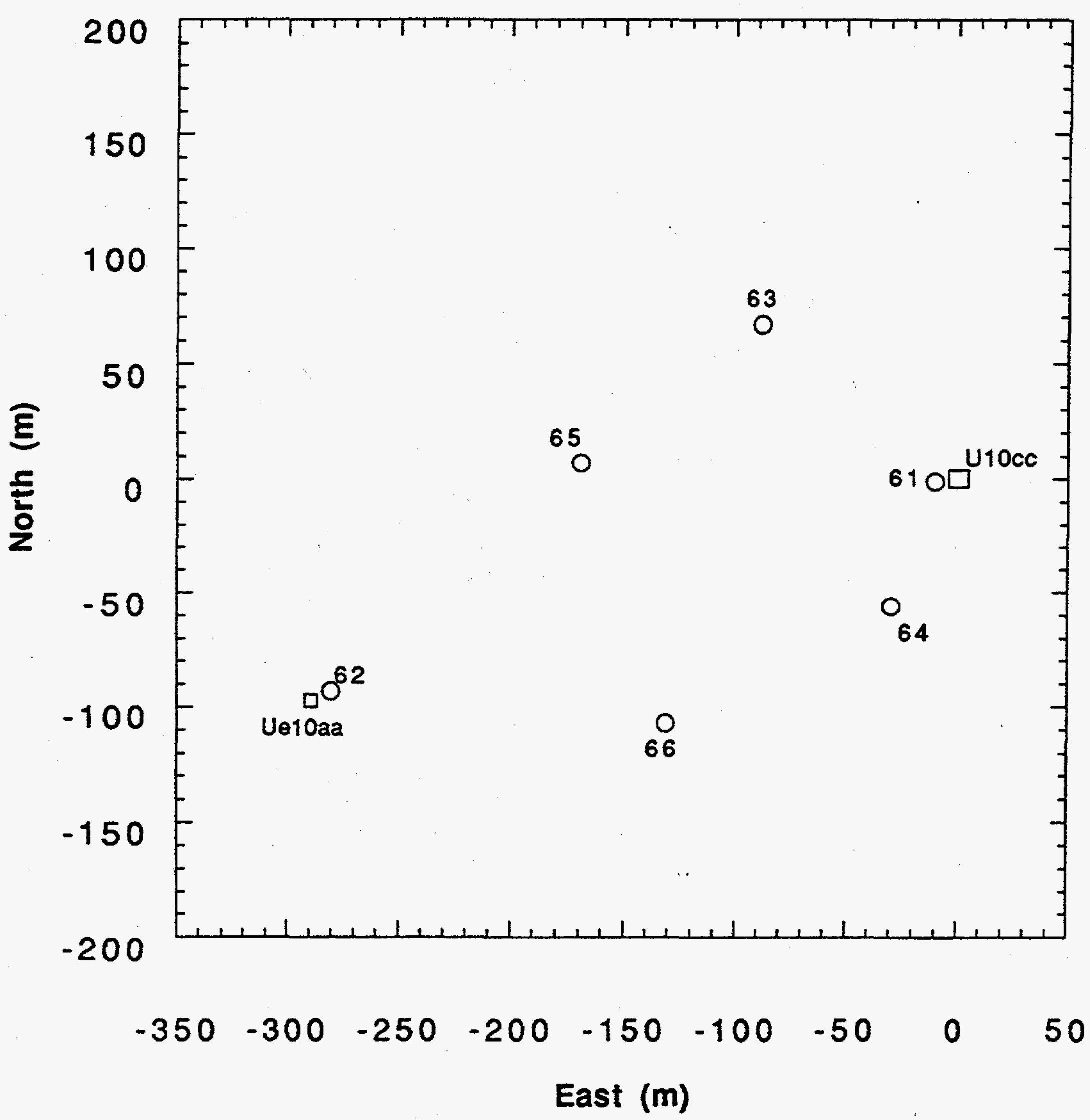


Figure 1.7 Plan view of the JARLSBERG surface array.

## 2. Emplacement

### 2.1. Pipe strain

Pre-shot, the pipe strain gauge is used to monitor the load on the emplacement pipe. The load upon landing was 82,500 pounds.

### 2.2. Plug level and temperature

A thermistor in the top plug monitored the plug temperature history which was observed in the stemming trailer. A satisfactory plug temperature history was a requirement for the completion of stemming of the hole. As of this writing, the actual histories of the TPE plugs temperature are not available.

No other emplacement data are available except through the stemming log of Holmes & Narver[3].

## 3. Stemming Performance

None of the channels serviced by the multiplexers fielded below the deepest plug survived the EMP, while both of the multiplexers above the TPE plug at the 105 m depth operated satisfactorily.

### 3.1 Pressure and Radiation

Stations 31 and 32 were inoperative pre-shot although they calibrated properly 60 seconds before the event. These stations were among those with multiplexers fielded below the deepest plug and thus yielded no information.

### 3.2 Stress and Strain

Stations 11–18 and 81 were among those with multiplexers fielded below the deepest plug and thus yielded no information. The only strain station which may have yielded valid data from the emplacement hole was 82. Figure 3.1 shows the explosion–induced strain histories measured in the deepest TPE plug.

### 3.3 Motion

The three Celesco displacement gauge records are shown in Figure 3.2. Both the time around detonation and the time around collapse are covered. Stations 1 and 3 are anchored to the emplacement pipe with their free ends placed in the stemming and the top plug, respectively.

The two stemming plugs were instrumented with both vertical acceleration and velocity gauges; the data from these are shown in Figures 3.3 and 3.4. Peak amplitudes and times-of-arrival are included in the summary table 3.1. Noise levels in the recording system tend to make the displacements derived from acceleration suspect.

Characteristics of the transducers are given in tables 3.2 and 3.3.

## 3.4 Collapse

Figure 3.4 shows the strain in the deepest plug monitored during collapse while the collapse–induced motions recorded at stations 21 and 22 are shown in figures 3.6 and 3.7.

Collapse was monitored by a cliper cable system (Station 92). Positions of the cable break are plotted as a function of time in Figure 3.8. Also included are records from the other stations showing collapse activity within the stemming column. Only the cliper data are plotted to scale, the other information merely indicates timing. Stations 21 and 22 are represented by the derived displacement while Station 82 (strain) is represented by its vertical component.

The sensor cables for stations 91 and 92 were used as "D" cables for monitoring the stemming procedures and as CLIPERs for monitoring cavity collapse. Station 92 was switched to standard CLIPER electronics at about 0.1 s after detonation for recording while station 91 was recorded as a "D" cable for times after detonation. Computer software for converting the "D" cable signal to CLIPER equivalent information has not been developed, thus the station 91 data are not presented.

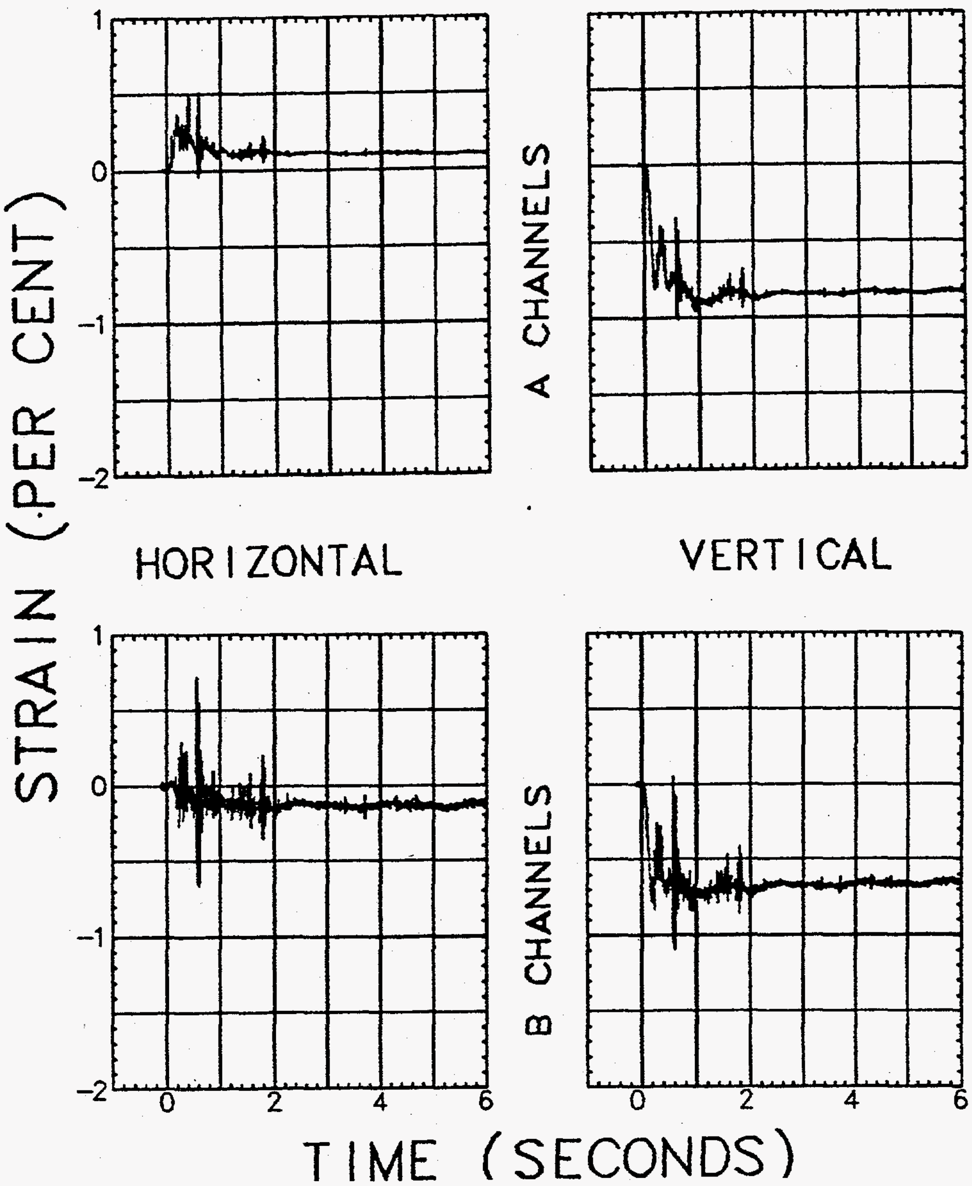


Figure 3.1 Explosion–induced horizontal and vertical strains measured in the TPE plug at a depth of 105 m (station 82).

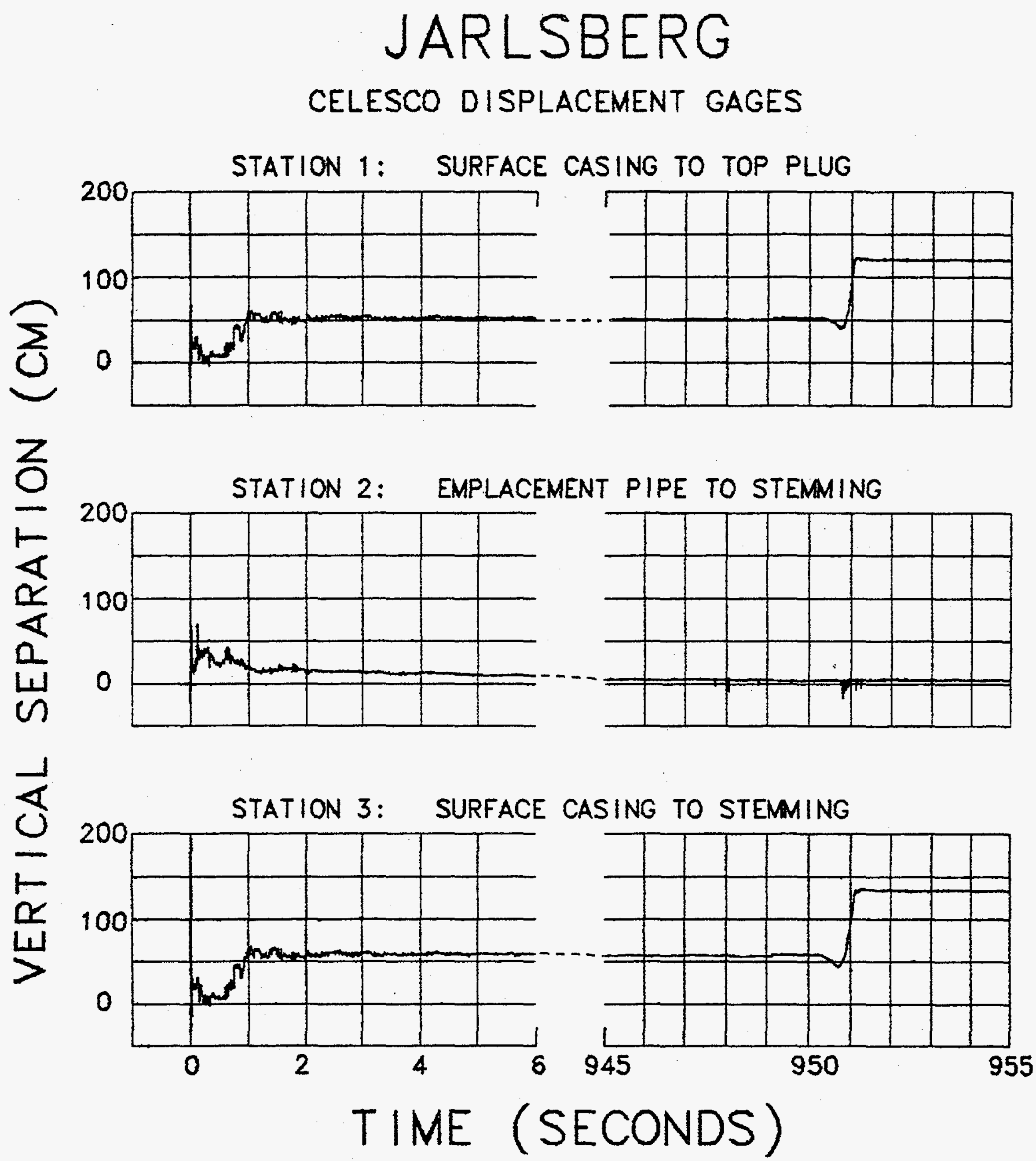


Figure 3.2. Relative displacement between surface casing, stemming and emplacement pipe, both during the explosion and subsequent collapse.

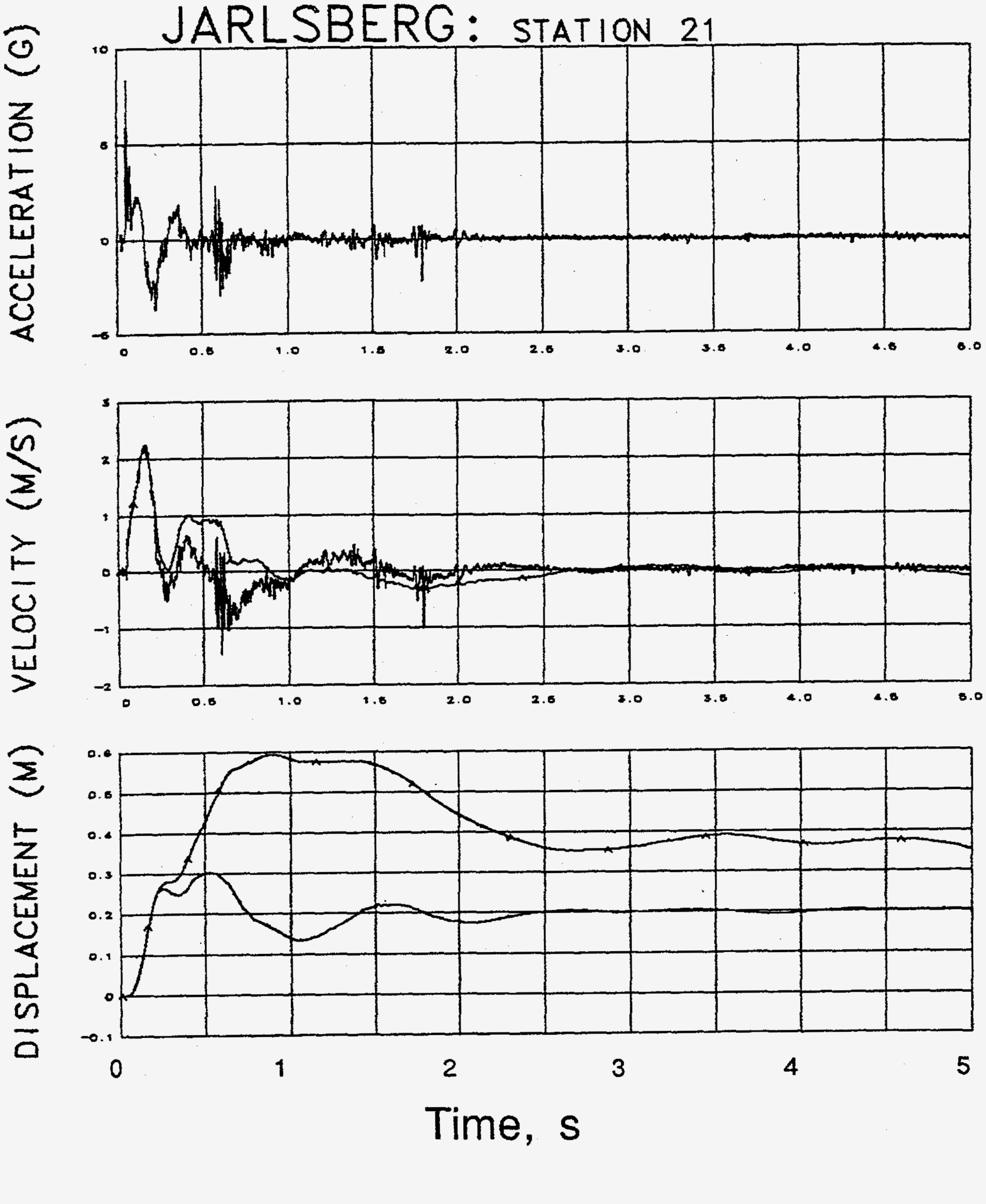


Figure 3.3. Explosion–induced vertical motion of the deepest TPE plug at a depth of 106 m (Station 21). Records annotated with "A" were derived from the accelerometer.

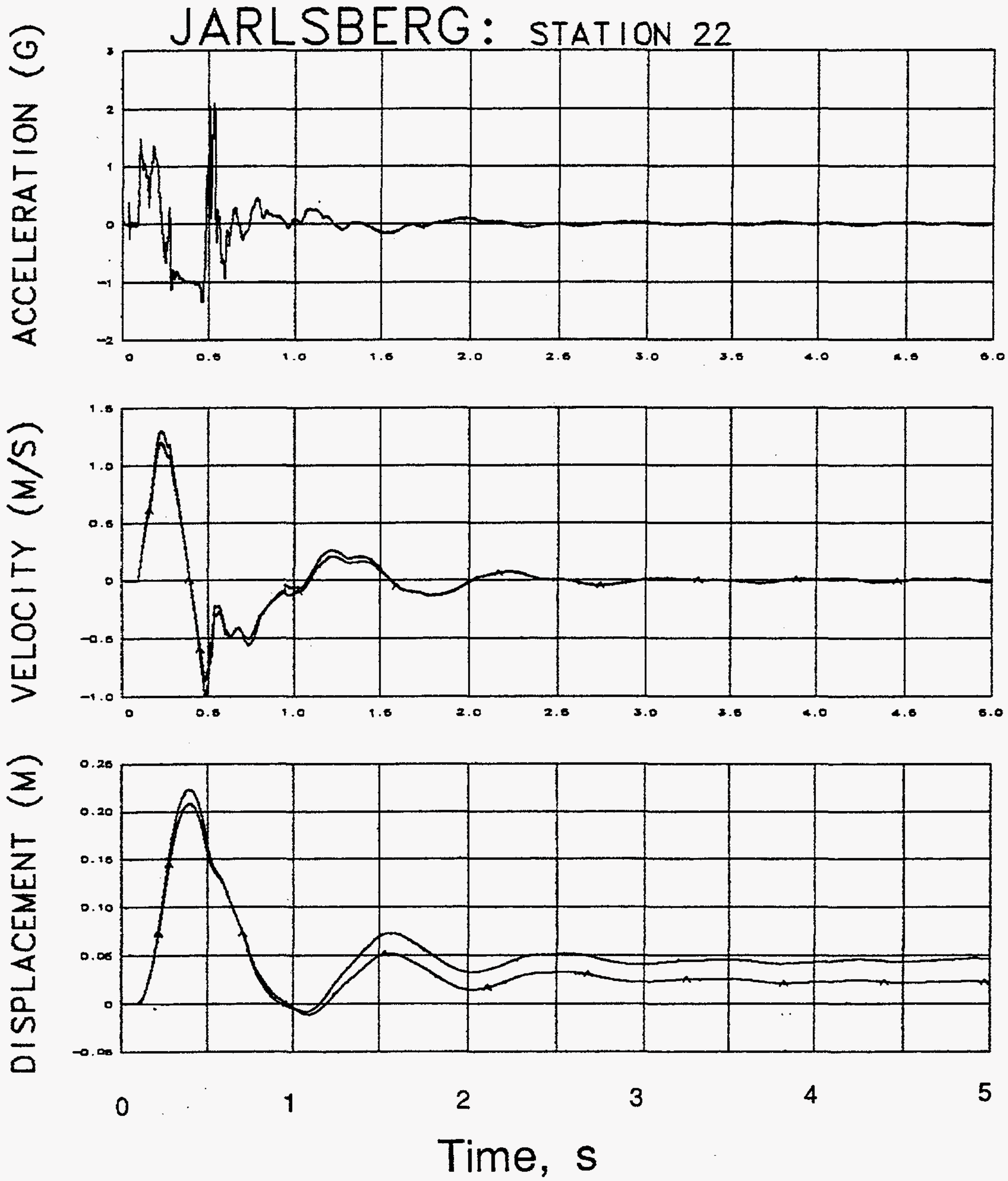


Figure 3.4. Explosion–induced vertical motion of the top TPE plug at a depth of 35 m (Station 22). Records annotated with "A" were derived from the accelerometer.

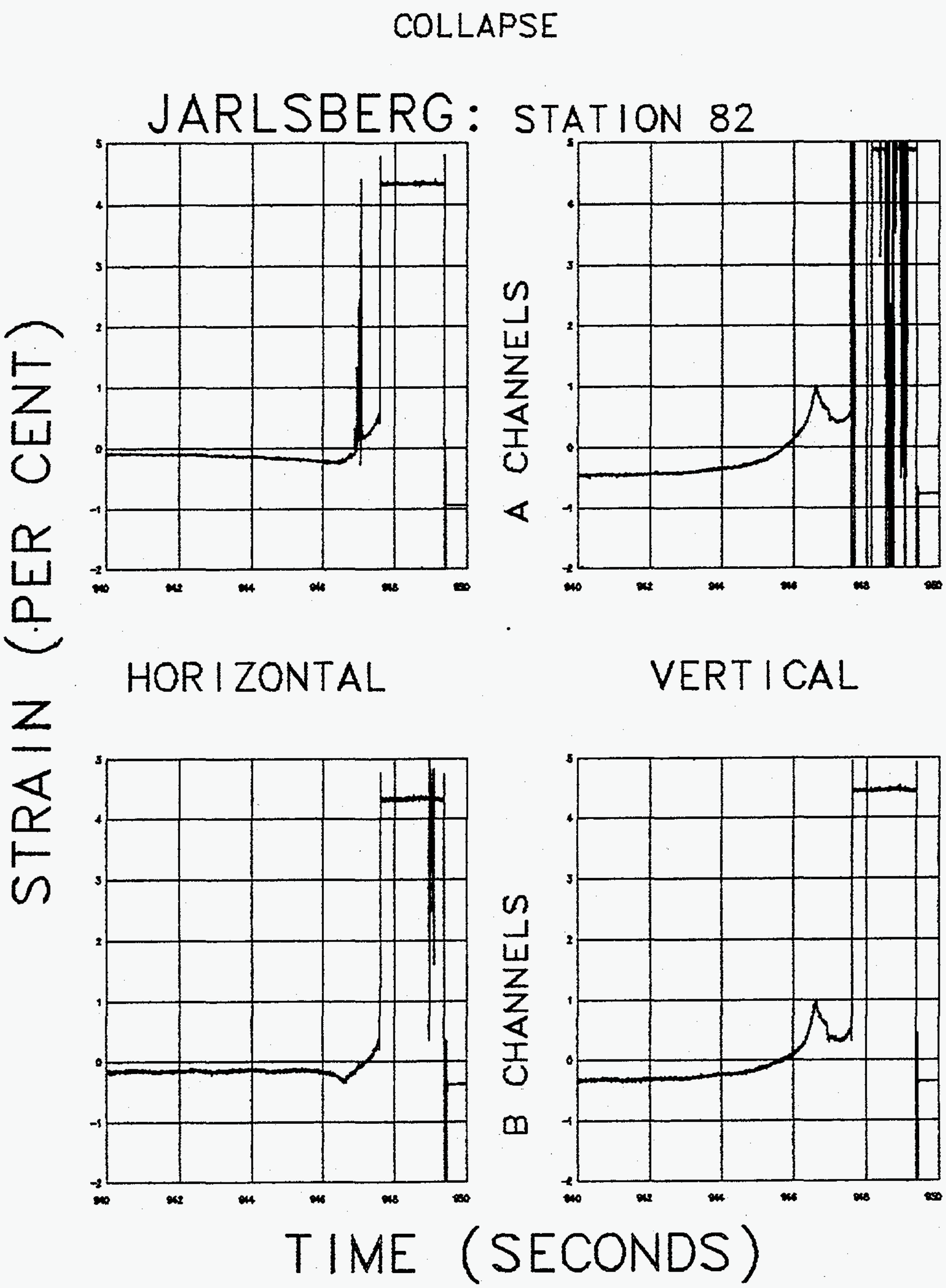


Figure 3.5. Collapse–induced horizontal and vertical strains measured in the TPE plug at a depth of 105 m (station 82).

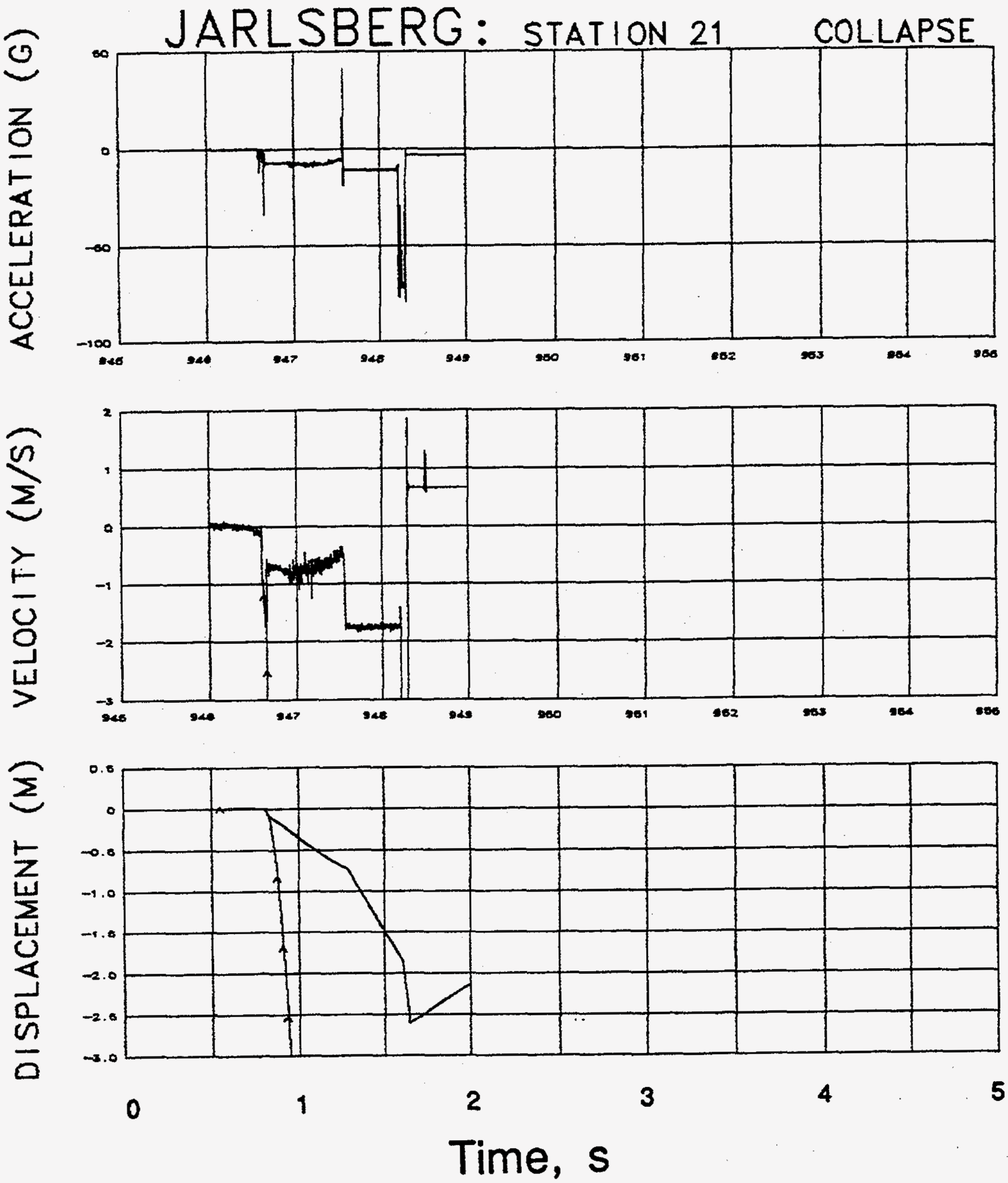


Figure 3.6. Collapse–induced vertical motion of the deepest TPE plug at a depth of 106 m (Station 21). Records annotated with "A" were derived from the accelerometer.

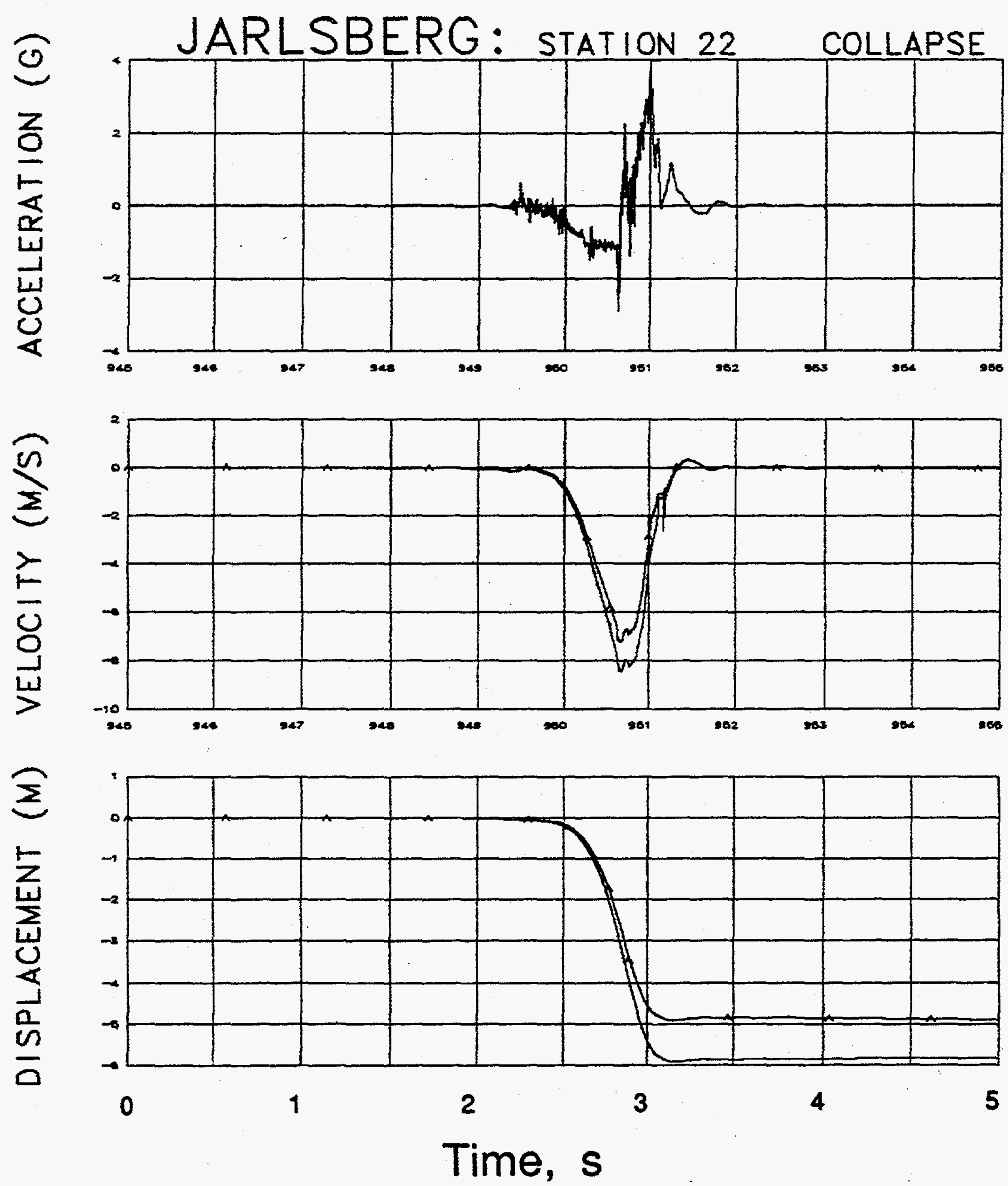


Figure 3.7. Collapse–induced vertical motion of the top TPE plug at a depth of 35 m (Station 22). Records annotated with "A" were derived from the accelerometer.

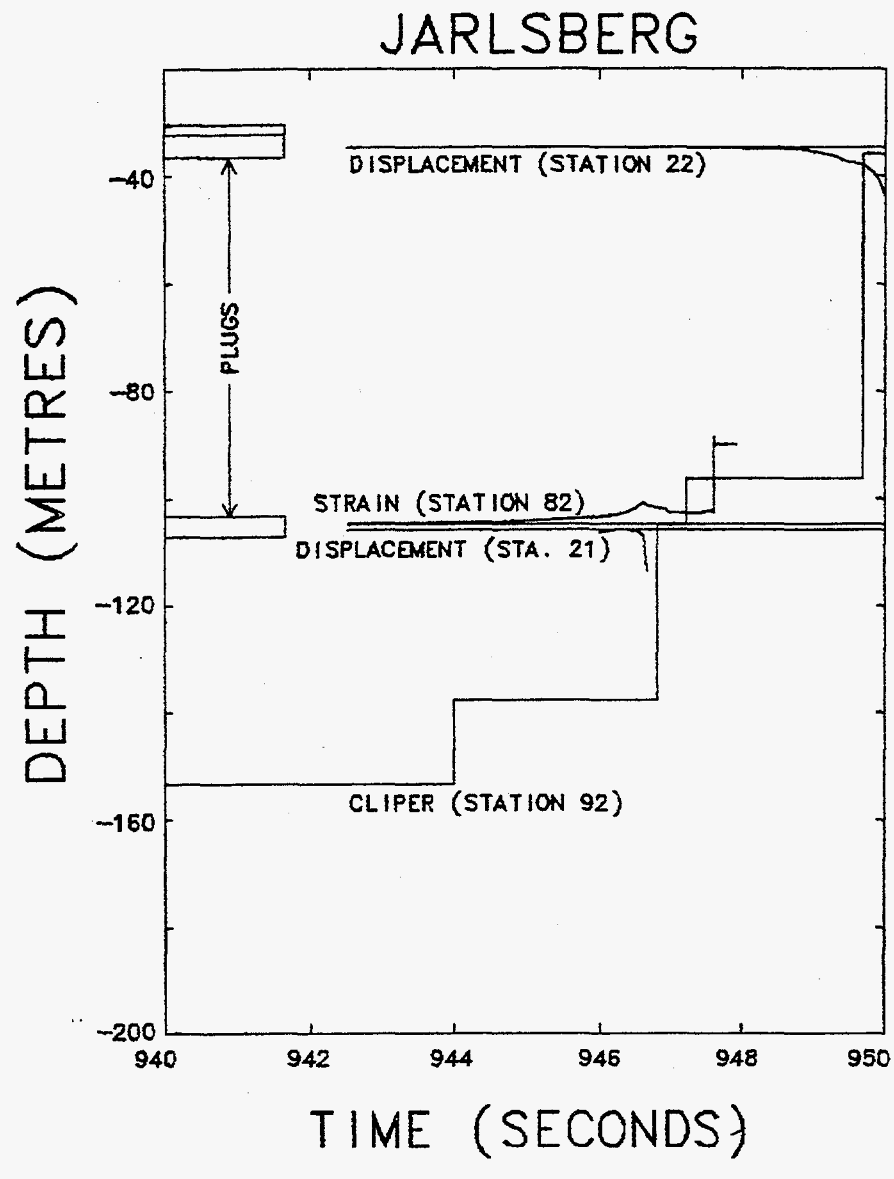


Figure 3.8. Collapse history as indicated by the CLIPER cable, motion stations in the TPE plugs, and the vertical strain measurement in the bottom plug.

## 4. Surface Motion

See Figure 1.7 for a lay-out of the relative positions of the surface array instrumentation.

All surface stations were instrumented with vertical accelerometers and velocity gauges and each contained a supplemental accelerometer denoted "gv" to identify it as one that is usually employed as a geophone oriented in the vertical direction. All of the "gv" gauges (except at station 62) were over-ranged and thus had "clipped" peaks. When shown with the data from velocity gauges, the velocity and displacement histories derived from the standard accelerometers are annotated with an "A". The histories obtained from the geophone accelerometers are annotated with a "B". All the surface motion histories, both measured and derived are presented in figures 4.1 through 4.6. All three transducers of Station 62 remained within band and are presented in Figure 4.2. As indicated in section 1.2, the velocity transducers for stations 64, 65, and 66 all malfunctioned at zero time and the records presented are thus derived from the accelerometer histories. The accelerometer at station 63 (channel 63av) was apparently damaged by the EMP and is also excluded.

All three channels of Station 61 were processed to yield the motion during collapse, (Figure 4.7). Although the plot is not precise enough to show it, 61gv indicates a "free-fall" period (negative acceleration of close to -1 g). This channel was severely clipped (the band-width was ±1.3 g) so the integrals from this channel should not be accepted.

A summary of the explosion-induced surface motion data is included in table 3.1 and the transducer characteristics are given in tables 3.2 and 3.3. Included in table 3.1 are the horizontal azimuthal directions of propagation from the working point to the respective stations.

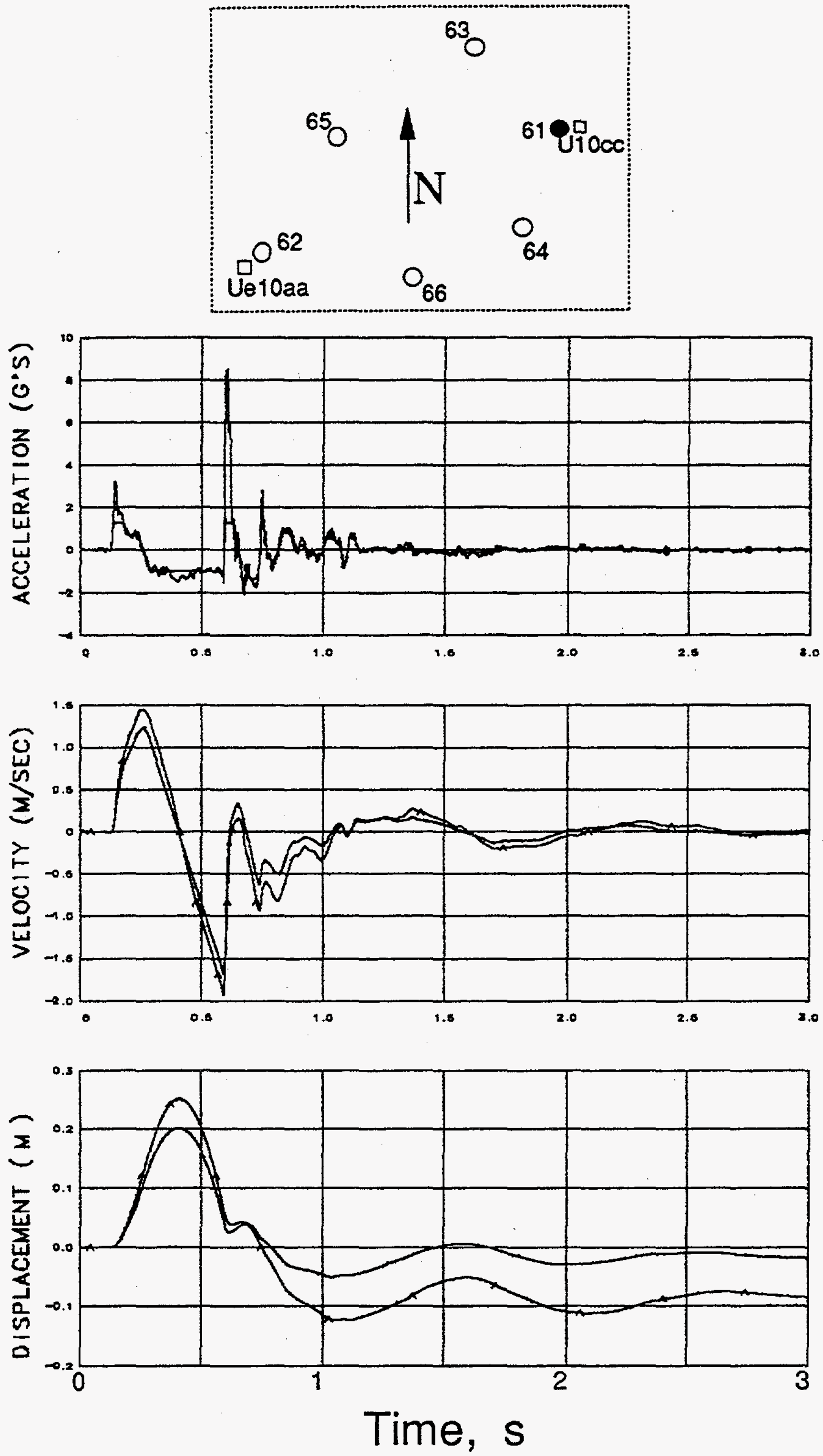


Figure 4.1 Explosion–induced vertical motion of the ground surface at a horizontal range of 10.1 m and azimuth of 187.0° from surface ground zero (station 61). Traces annotated with "A" were derived from the accelerometer.

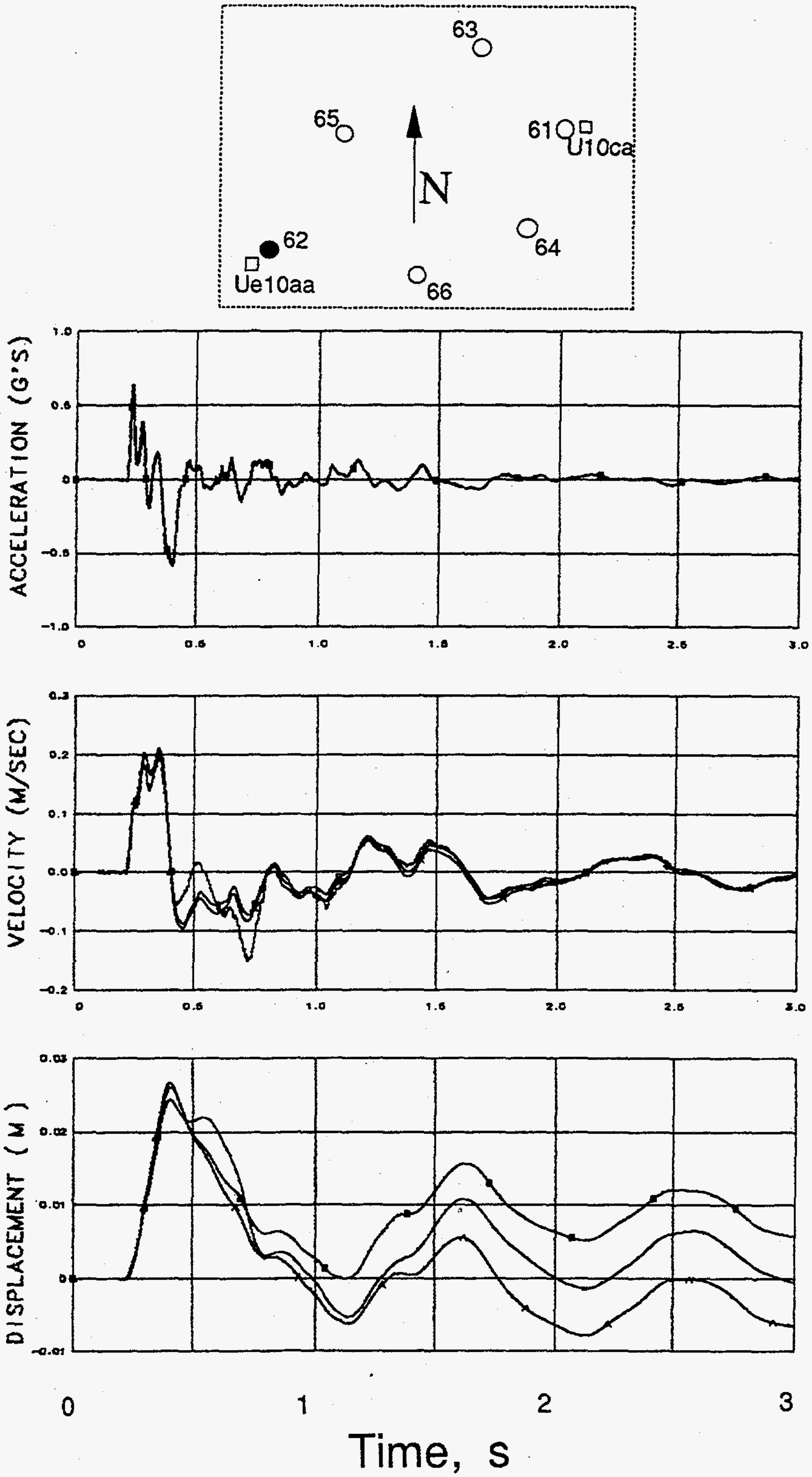


Figure 4.2. Explosion–induced vertical motion of the ground surface at a horizontal range of 295.1 m and azimuth of 198.4° from surface ground zero (station 62). Traces annotated with "A" were derived from the accelerometer. Traces annotated with "B" were derived from the supplemental accelerometer.

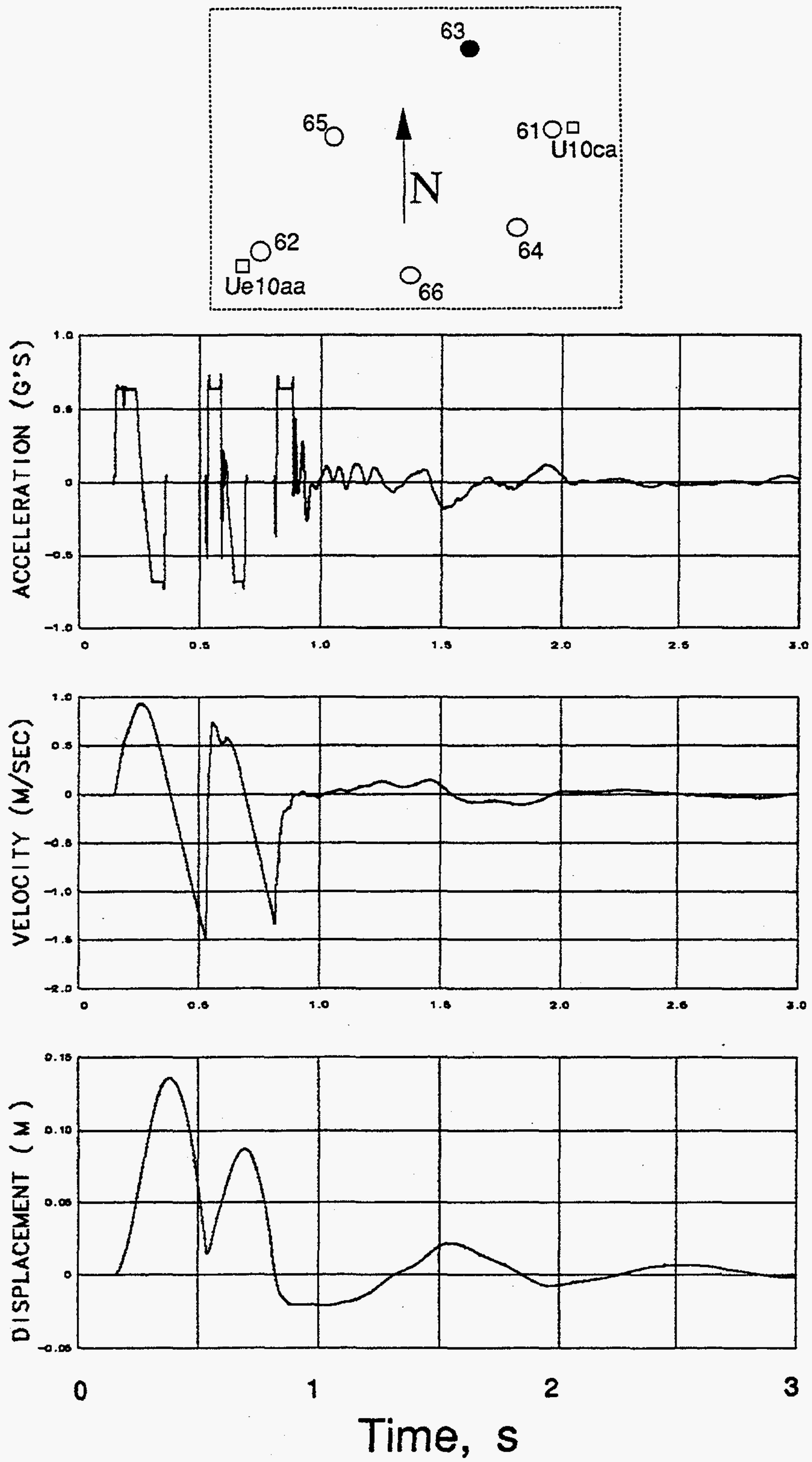


Figure 4.3. Explosion–induced vertical motion of the ground surface at a horizontal range of 110.5 m and azimuth of 142.8° from surface ground zero (station 63).

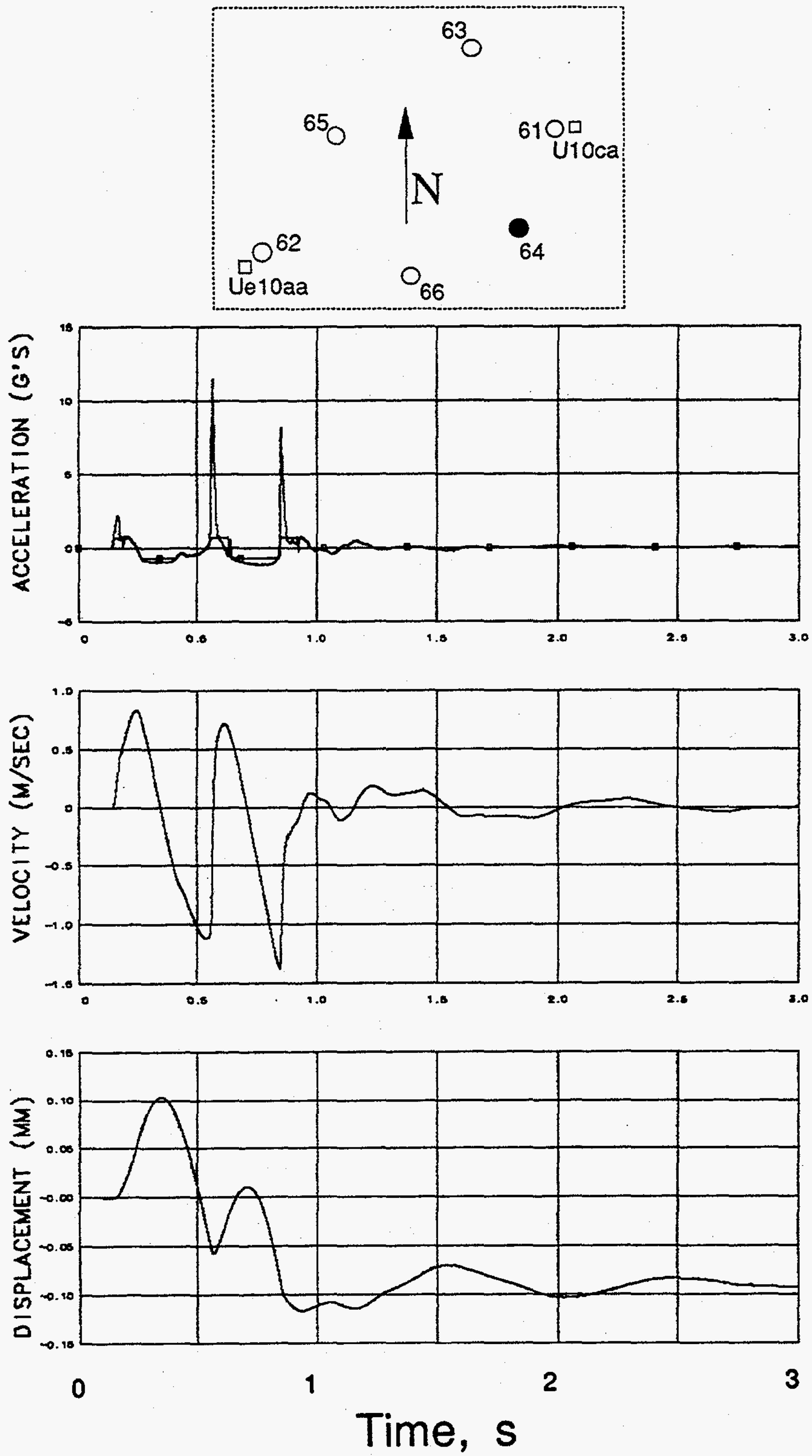


Figure 4.4. Explosion–induced vertical motion of the ground surface at a horizontal range of 63.2 m and azimuth of 242.7° from surface ground zero (station 64). Traces annotated with "B" were derived from the supplemental accelerometer.

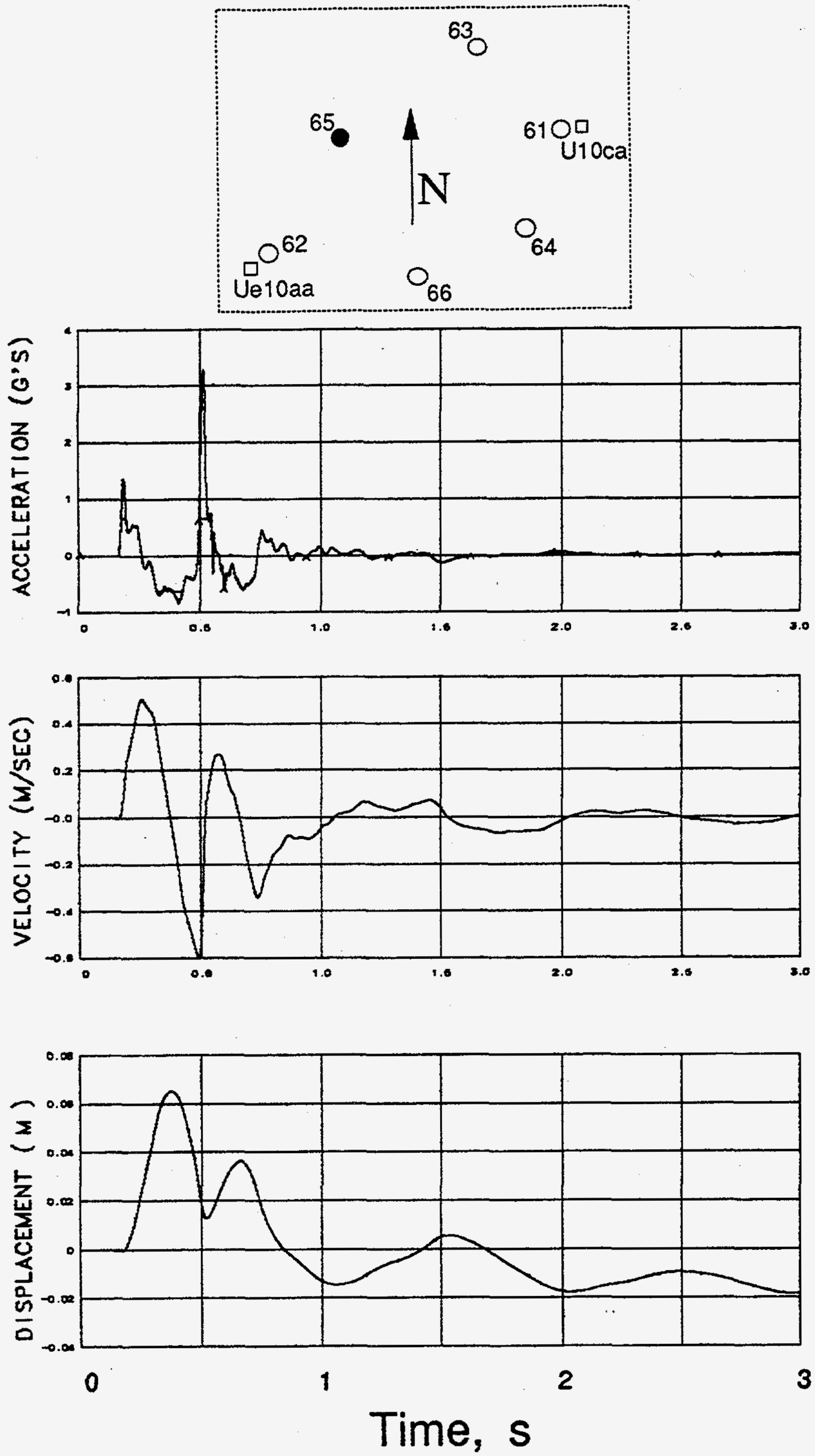


Figure 4.5 Explosion–induced vertical motion of the ground surface at a horizontal range of 180.6 m and azimuth of 177.7° from surface ground zero (station 65). Traces annotated with "A" were derived from the supplemental accelerometer.

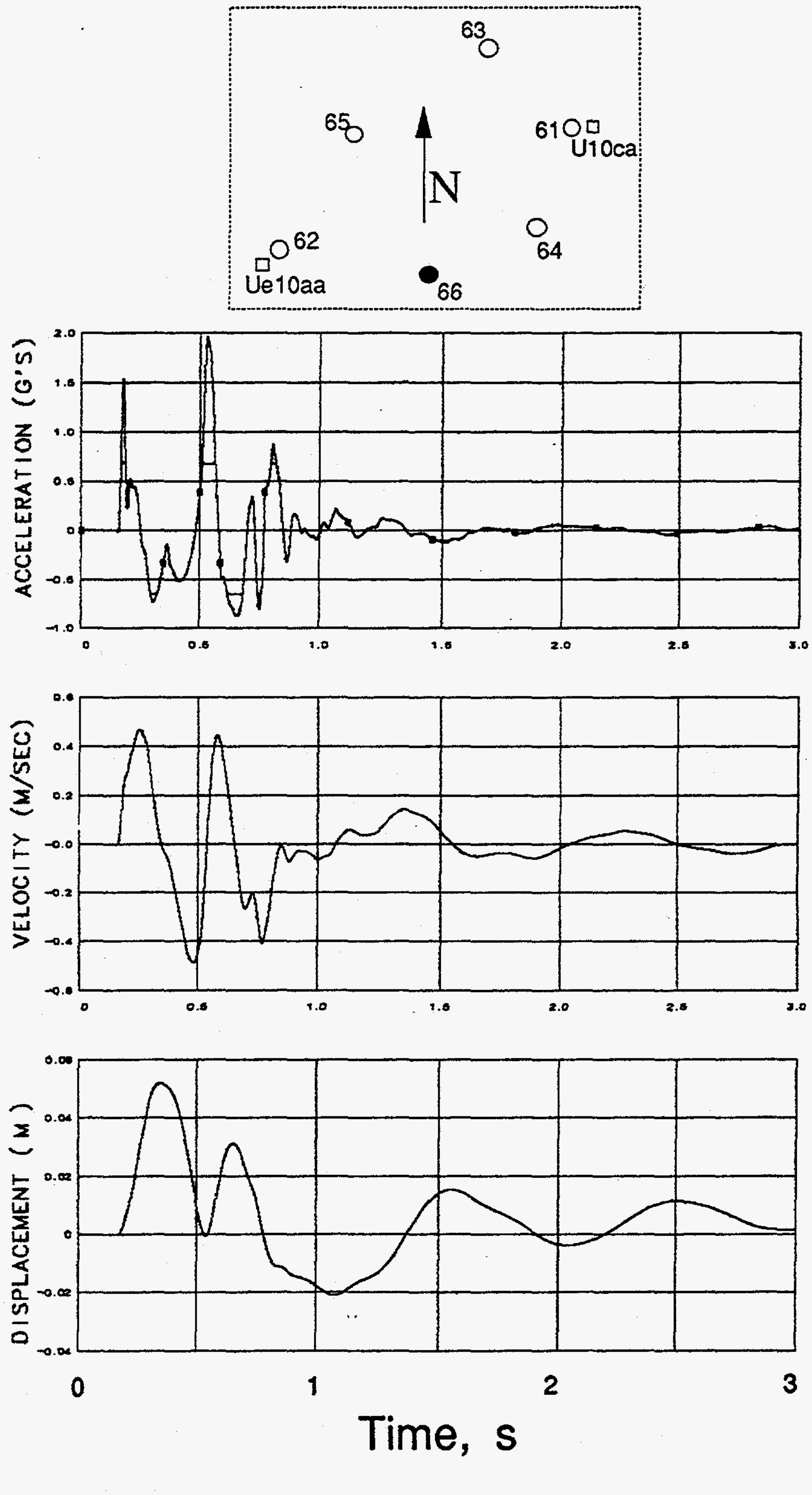


Figure 4.6 Explosion–induced vertical motion of the ground surface at a horizontal range of 169.3 m and azimuth of 219.3° from surface ground zero (station 66). Traces annotated with "B" were derived from the supplemental accelerometer.

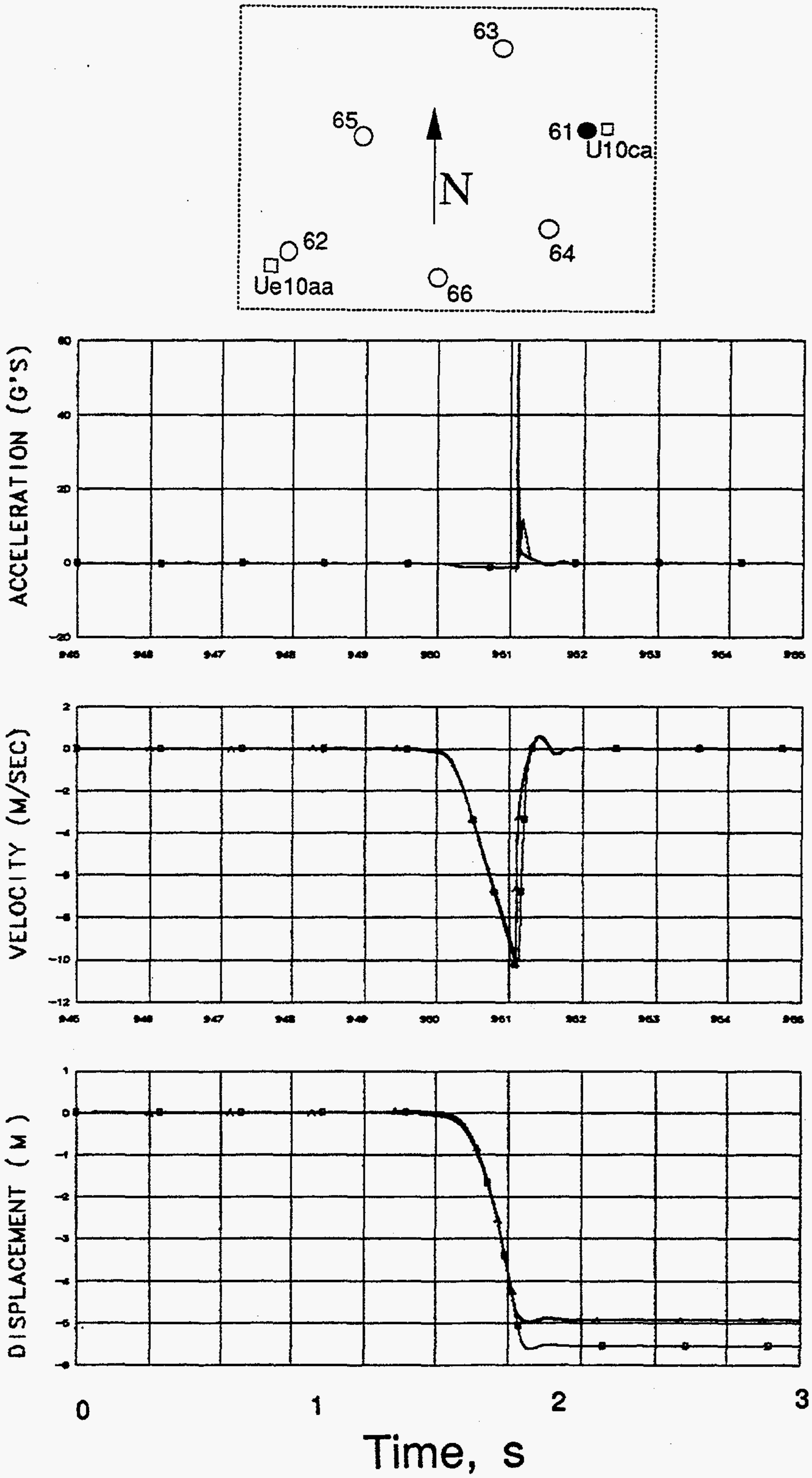


Figure 4.7. Collapse–induced vertical motion of the ground surface at a horizontal range of 10.1 m and azimuth of 187° from surface ground zero (station 61). Traces annotated with "A" were derived from the accelerometer. Traces annotated with "B" were derived from the supplemental accelerometer.

# Table 3.1

## Surface and Emplacement Hole Motion Summary

| Gauge | Slant Range (m) | Azimuth† angle (degrees) | Arrival Time (ms) | Peak Acceleration (g) | Peak Velocity (m/s) | Peak Displacement (m) | Residual Displacement (cm) |
|---|---|---|---|---|---|---|---|
| 21av | 94.0 | NA | 19[a], 45 | 8.3 | 2.25 | 0.280 | (b) |
| 21uv | | | | | 2.20 | 0.265 | 200 |
| 22av | 165.4 | NA | 35(a), 91 | 1.46 | 1.20 | 0.207 | 24 |
| 22uv | | | | | 1.30 | 0.223 | 45 |
| 61gv | (c) | | | | | | |
| 61av | 210.6 | 187.0 | 125 | 2.9, 12.1[d] | 1.35 | 0.234 | (b) |
| 61uv | | | | | 1.24 | 0.204 | -15 |
| 62gv | | | 166, 241 | 0.630 | 0.200 | 0.0260 | 9 |
| 62av | 324.7 | 198.4 | 213 | 0.628 | 0.203 | 0.0265 | -2 |
| 62uv | | | | | 0.181 | 0.0243 | 2 |
| 63gv | (c) | | | | | | |
| 63av | 242.3 | 142.8 | 145 | (e) | | | |
| 63uv | | | | | 0.830 | 0.136 | 1 |
| 64gv | (c) | | - | - | 3.75 | 2.00 | (b) |
| 64av | 242.3 | 242.7 | 135 | 2.15, 11.5[d] | 0.820 | 0.103 | -90 |
| 64uv | (e) | | - | - | | | |
| 65gv | (c) | | | | | | |
| 65av | 278.3 | 177.7 | 166 | 1.36, 3.27(d) | 0.505 | 0.065 | -17 |
| 65uv | (e) | | | | 1.77 | | |
| 66gv | (c) | | - | - | | | |
| 66av | 278.5 | 219.3 | 154 | 1.53, 1.95[d] | 0.465 | 0.052 | 3 |
| 66uv | (e) | | | | | | |

† Horizontal angle of propagation from the working point; zero = East
(a) emplacement pipe-induced arrival
(b) invalid data
(c) peaks invalid: data out of band
(d) slap-down peak
(e) malfunction; reason unknown

## Table 3.2

## Surface Array & Emplacement Hole Accelerometer Characteristics

| Gauge | Natural Frequency (Hz) | Damping Ratio | System Range (g) | type † |
|---|---|---|---|---|
| 21av | NA | NA | 80 | vr |
| 22av | 410 | 0.65 | 16 | vr |
| 61av | 570 | 0.65 | 30.0 | vr |
| 61gv | 253 | NA | 1.0 | pr |
| 62av | 260 | 0.62 | 3.0 | vr |
| 62gv | 250 | NA | 0.5 | pr |
| 63av | 267 | 0.65 | 4.0 | vr |
| 63gv | 250 | NA | 0.5 | pr |
| 64av | 260 | 0.65 | 4.0 | vr |
| 64gv | 252 | NA | 0.5 | pr |
| 65av | 170 | 0.60 | 3.0 | vr |
| 65gv | 254 | NA | 0.5 | pr |
| 66av | 170 | 0.70 | 3.0 | vr |
| 66gv | 253 | NA | 0.5 | pr |

† pr = Piezoresitive; vr = variable reluctance

## Table 3.3

**Surface Array & Emplacement Hole Velocimeter Characteristics**

| Gauge | Natural Frequency (Hz) | Time to 0.5 Amplitude (s) | Calibration Temperature (°C) | Operate Temperature (°C) | System Range (m/s) |
|---|---|---|---|---|---|
| 21uv | NA | 11.3 | 24.2 | NA | 16.0 |
| 22uv | 3.558 | 7.30 | 23.31 | 42.17 | 8.0 |
| 61uv | 3.473 | 9.63 | 23.52 | 23.30 | 9.0 |
| 62uv | 3.519 | 8.61 | 24.46 | 22.37 | 2.0 |
| 63uv | 3.558 | 9.00 | 23.53 | 22.05 | 3.0 |
| 64uv | 3.645 | 7.94 | 23.68 | 21.32 | 3.0 |
| 65uv | 3.450 | 9.71 | 24.02 | 20.89 | 2.0 |
| 66uv | 3.606 | 8.05 | 24.90 | 19.71 | 2.0 |

## 5. Satellite Hole (Free-Field) Measurements

### 5.1 Motion

Data from all of the reporting stations are seen in Figures 5.1 through 5.21. Stations 42 and 43 were lost before the event and thus are not shown.

A summary of the explosion–induced free–field motion data is included in Table 5.1. Tables 5.2 and 5.3 list the characteristics of the motion transducers fielded in the satellite hole U10aa.

### 5.2 Stress (soil pressure)

Only station 54 appeared operational, however the signals received from stations 5154 are shown in figure 5.22. Stations 55 and 56 were inoperative pre–shot and not recorded.

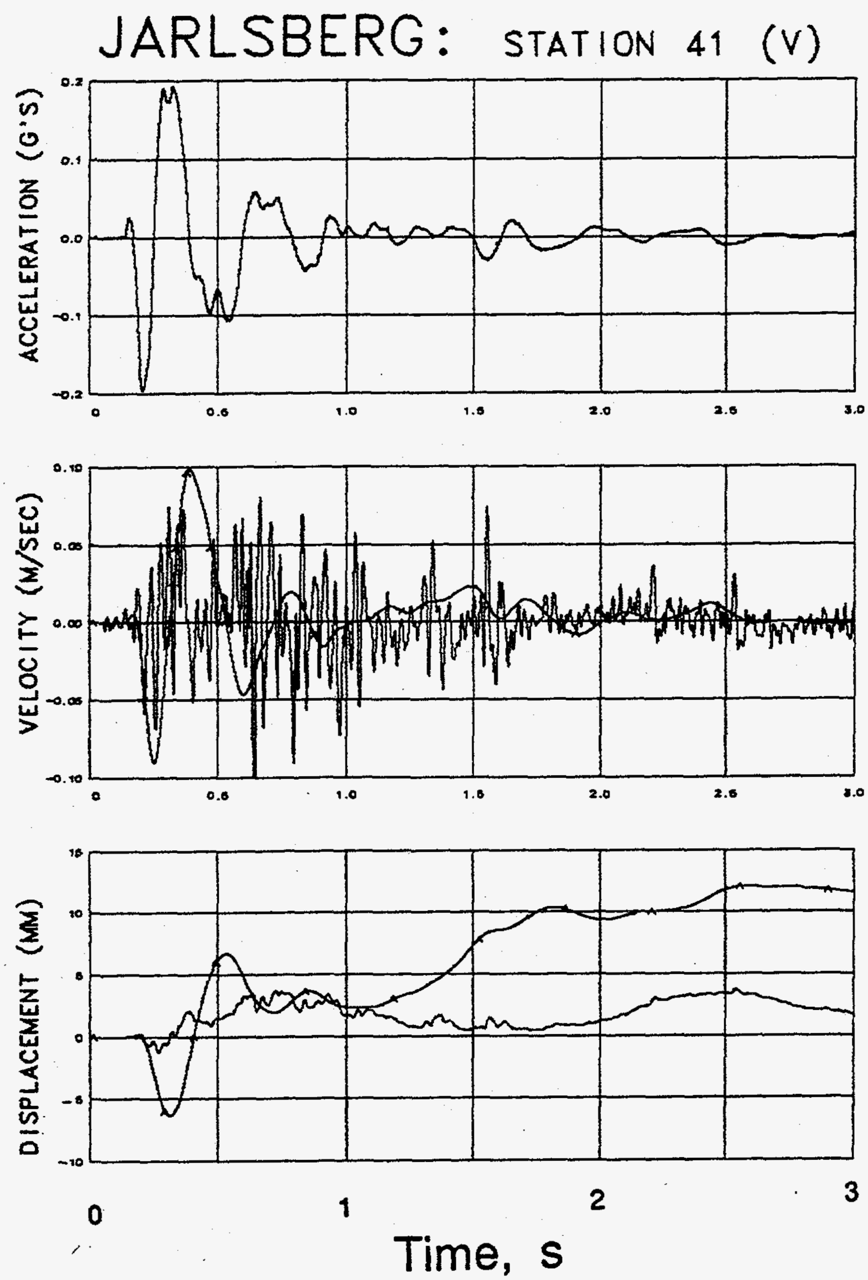


Figure 5.1 Explosion–induced vertical motion at a depth of 384 m in hole Ue10aa (station 41). Traces annotated with "A" were derived from the accelerometer.

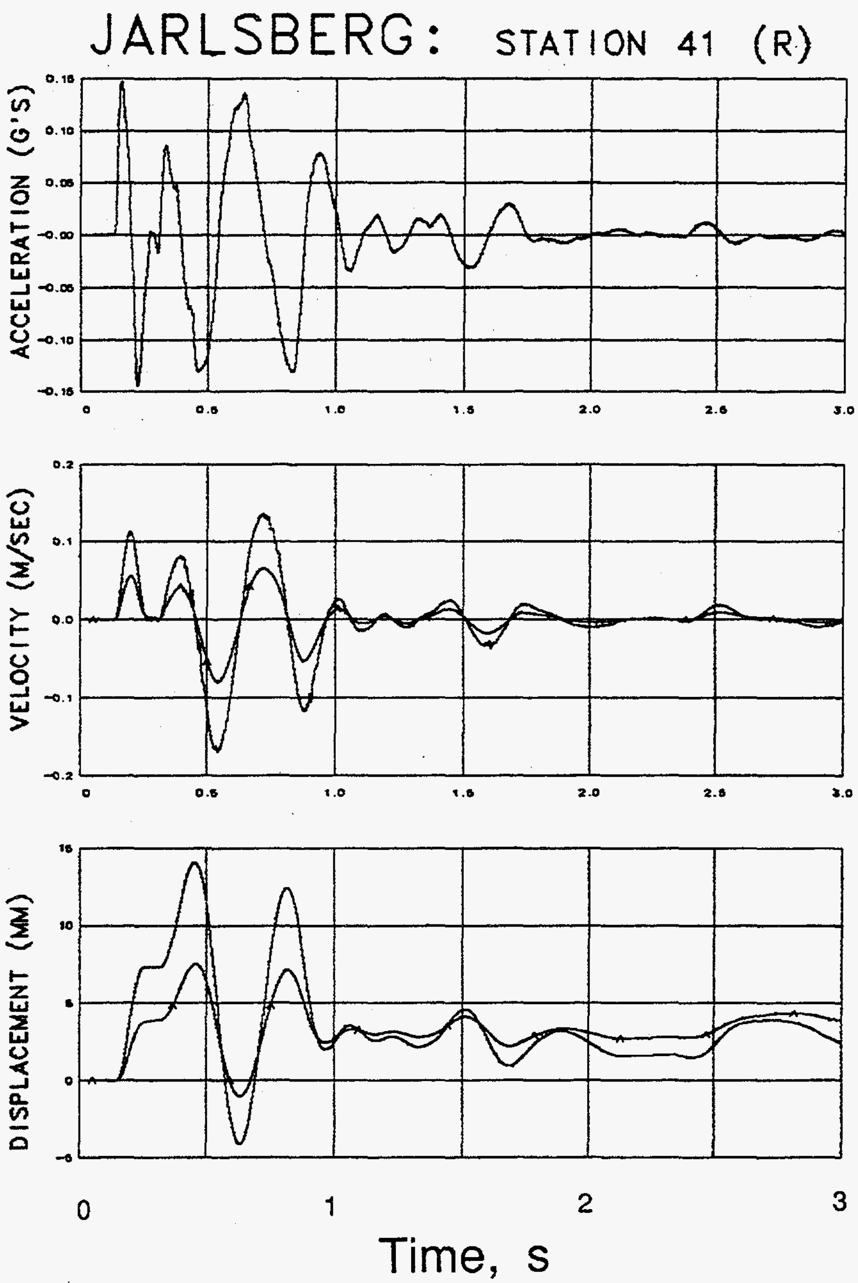


Figure 5.2 Explosion–induced radial–horizontal motion at a depth of 384 m in hole Ue10aa (station 41). Traces annotated with "A" were derived from the accelerometer.

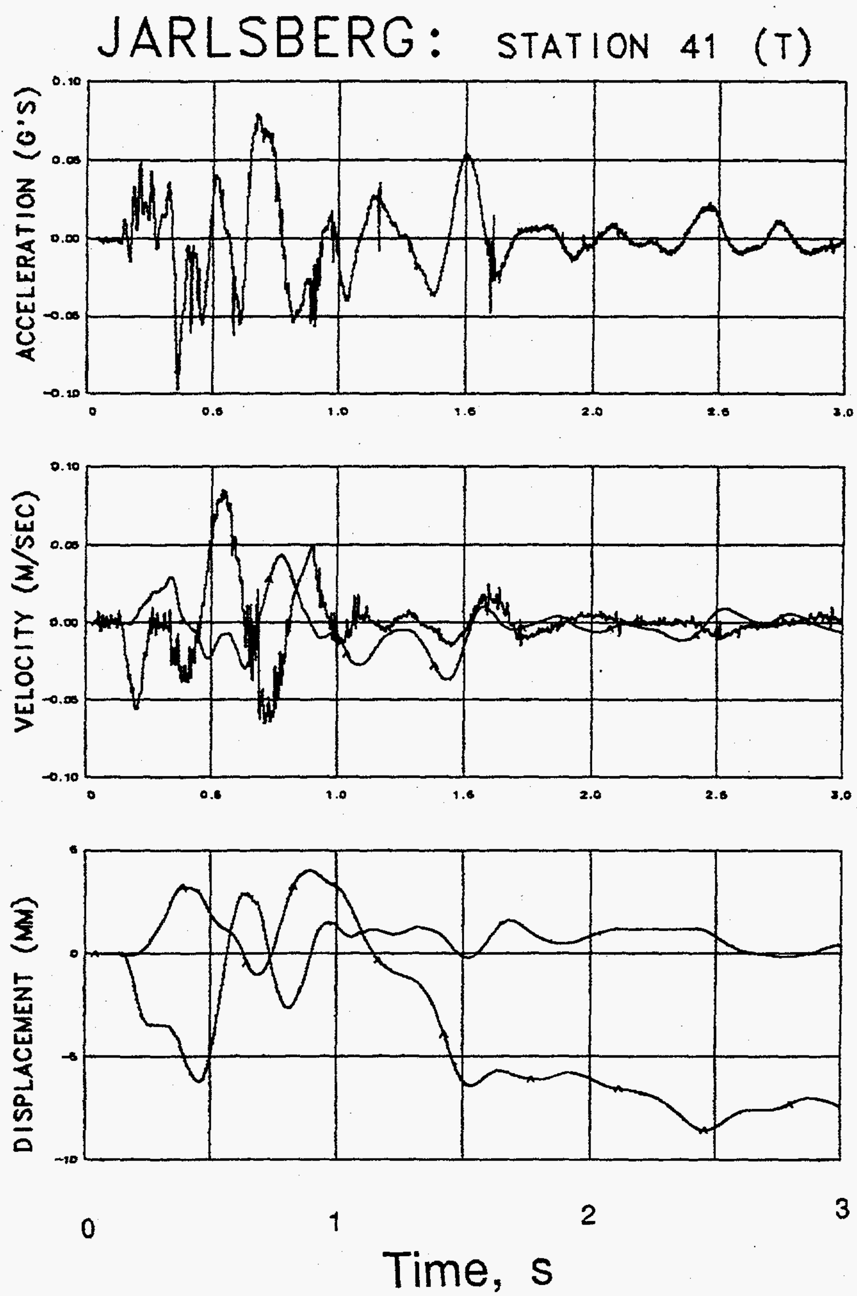


Figure 5.3 Explosion–induced transverse–horizontal motion at a depth of 384 m in hole Ue10aa (station 41). Traces annotated with "A" were derived from the accelerometer. Comparison of these data with those of figures 5.6 and 5.9 leads to the conclusion that the data from the transverse accelerometer at this station is likely invalid.

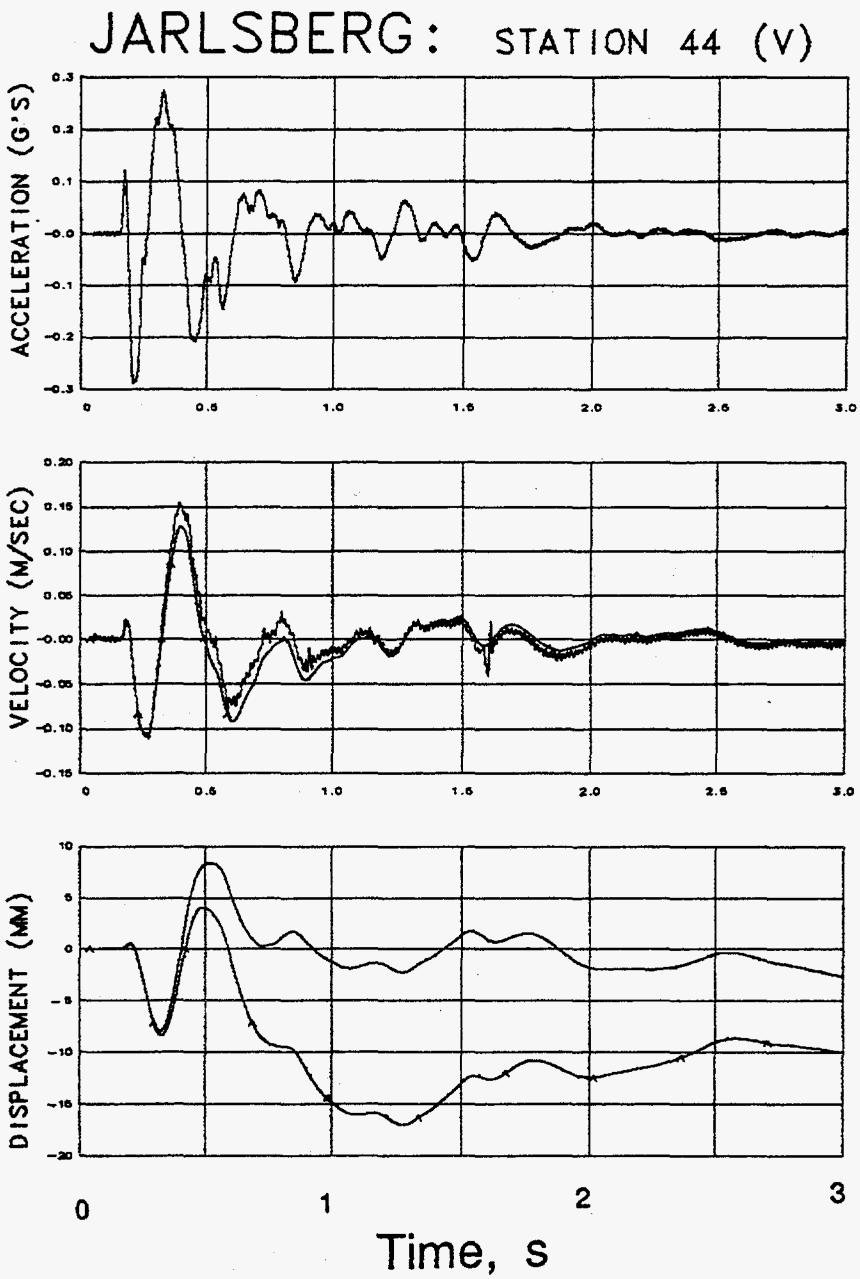


Figure 5.4 Explosion–induced vertical motion at a depth of 304 m in hole Ue10aa (station 44). Traces annotated with "A" were derived from the accelerometer.

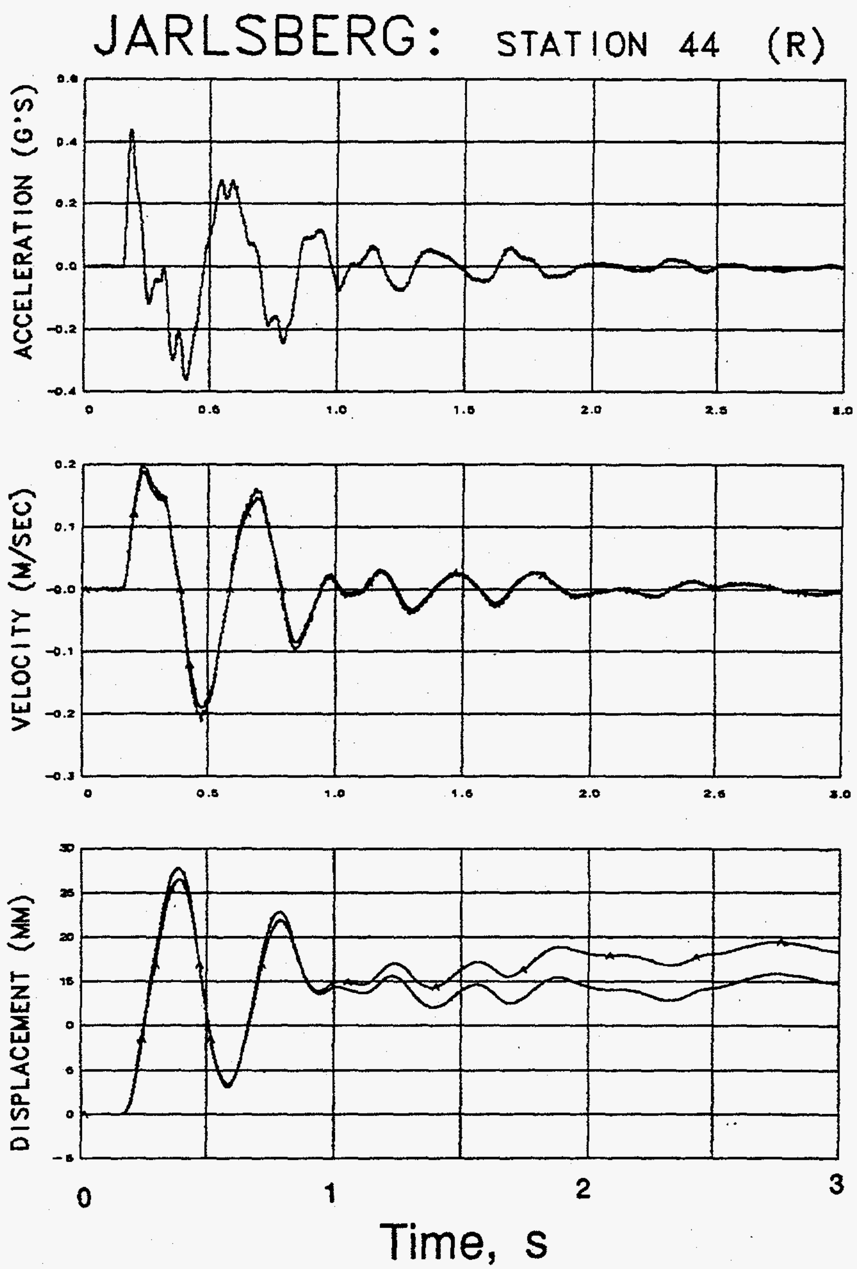


Figure 5.5 Explosion–induced radial–horizontal motion at a depth of 304 m in hole Ue10aa (station 44). Traces annotated with "A" were derived from the accelerometer.

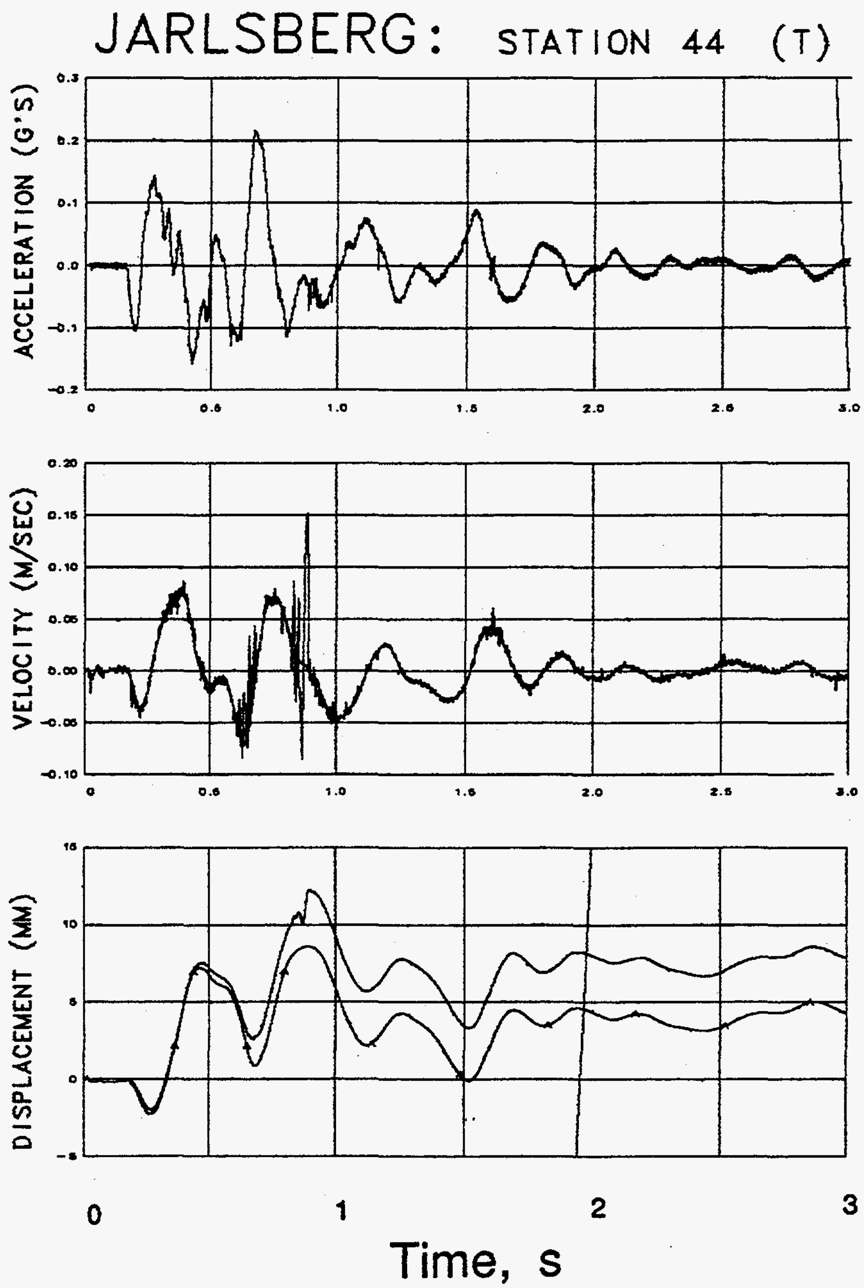


Figure 5.6 Explosion–induced transverse–horizontal motion at a depth of 304 m in hole Ue10aa (station 44). Traces annotated with "A" were derived from the accelerometer.

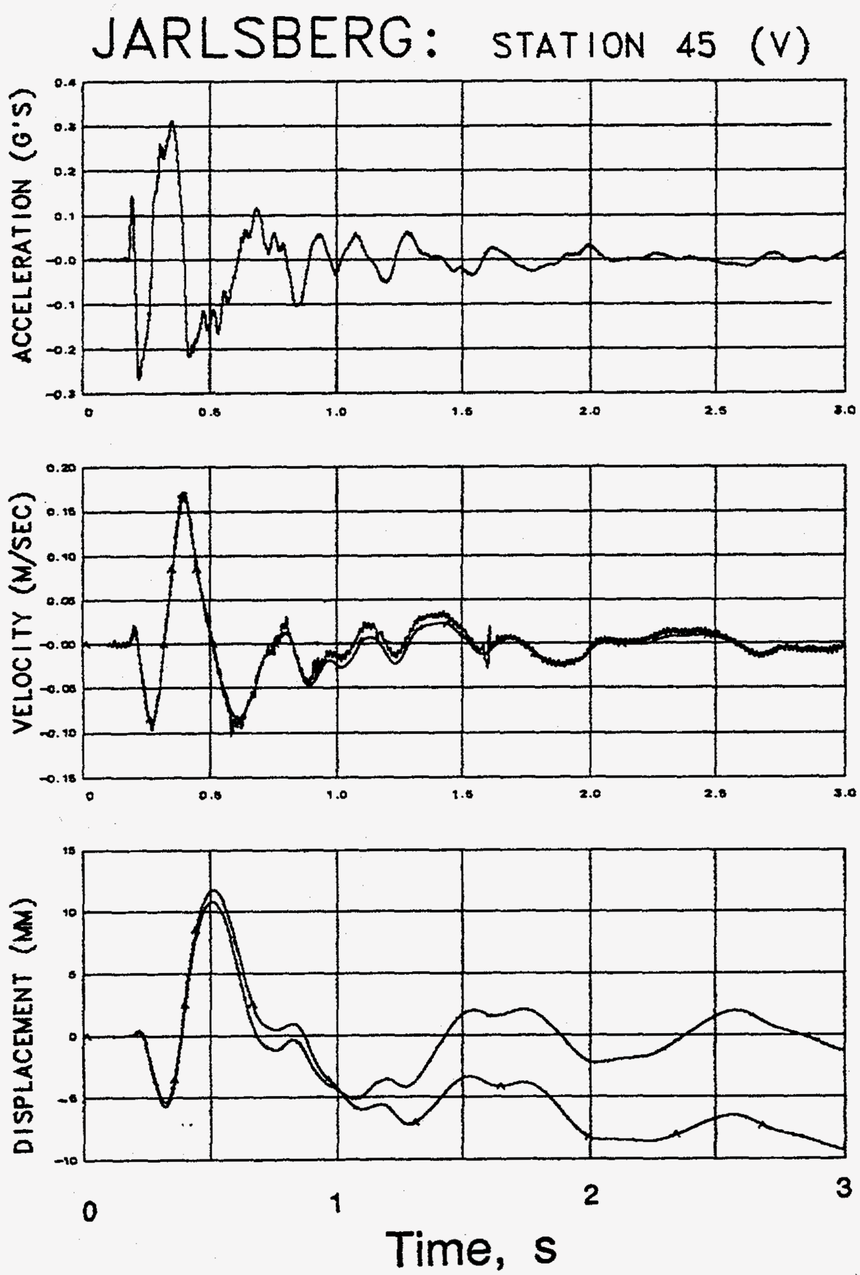


Figure 5.7 Explosion–induced vertical motion at a depth of 251m in hole Ue10aa (station 45). Traces annotated with "A" were derived from the accelerometer.

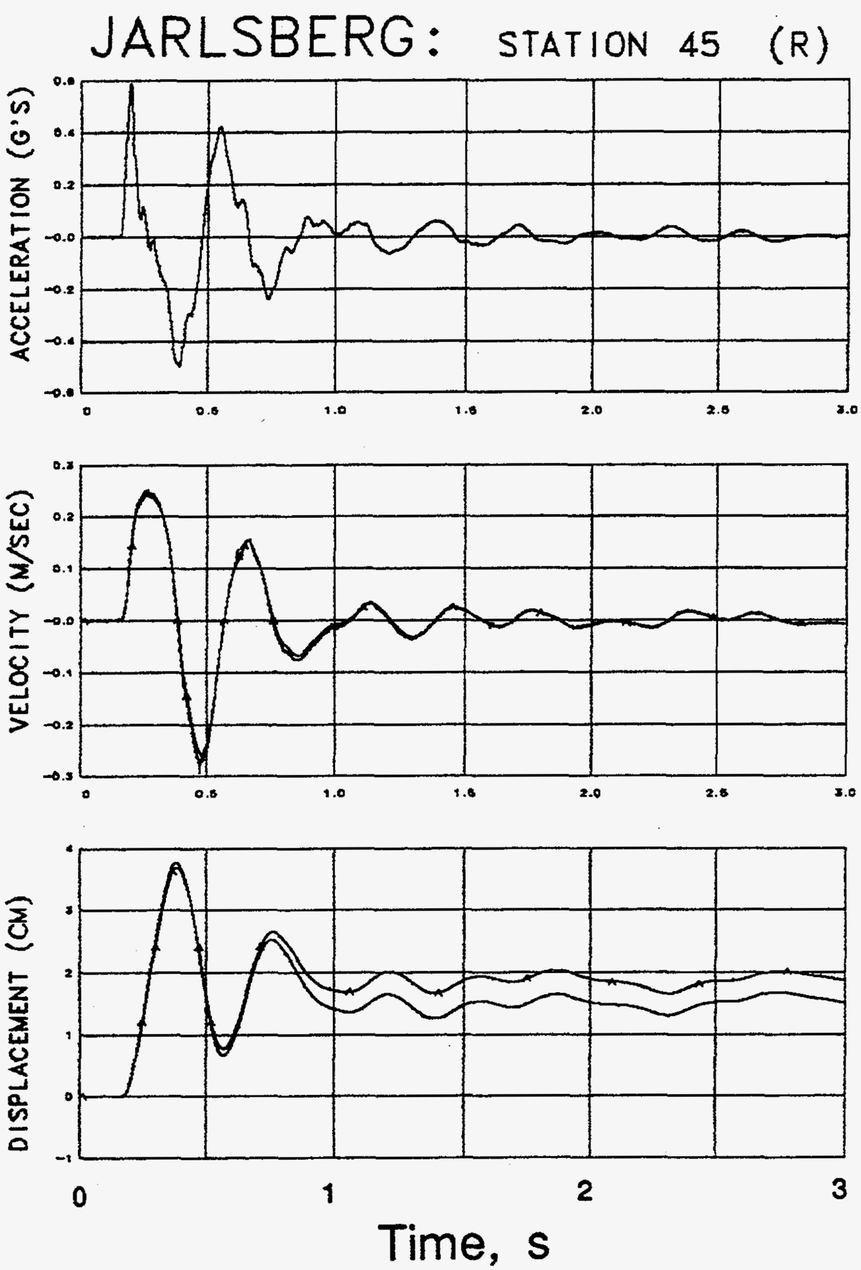


Figure 5.8 Explosion–induced radial–horizontal motion at a depth of 251 m in hole Ue10aa (station 45). Traces annotated with "A" were derived from the accelerometer.

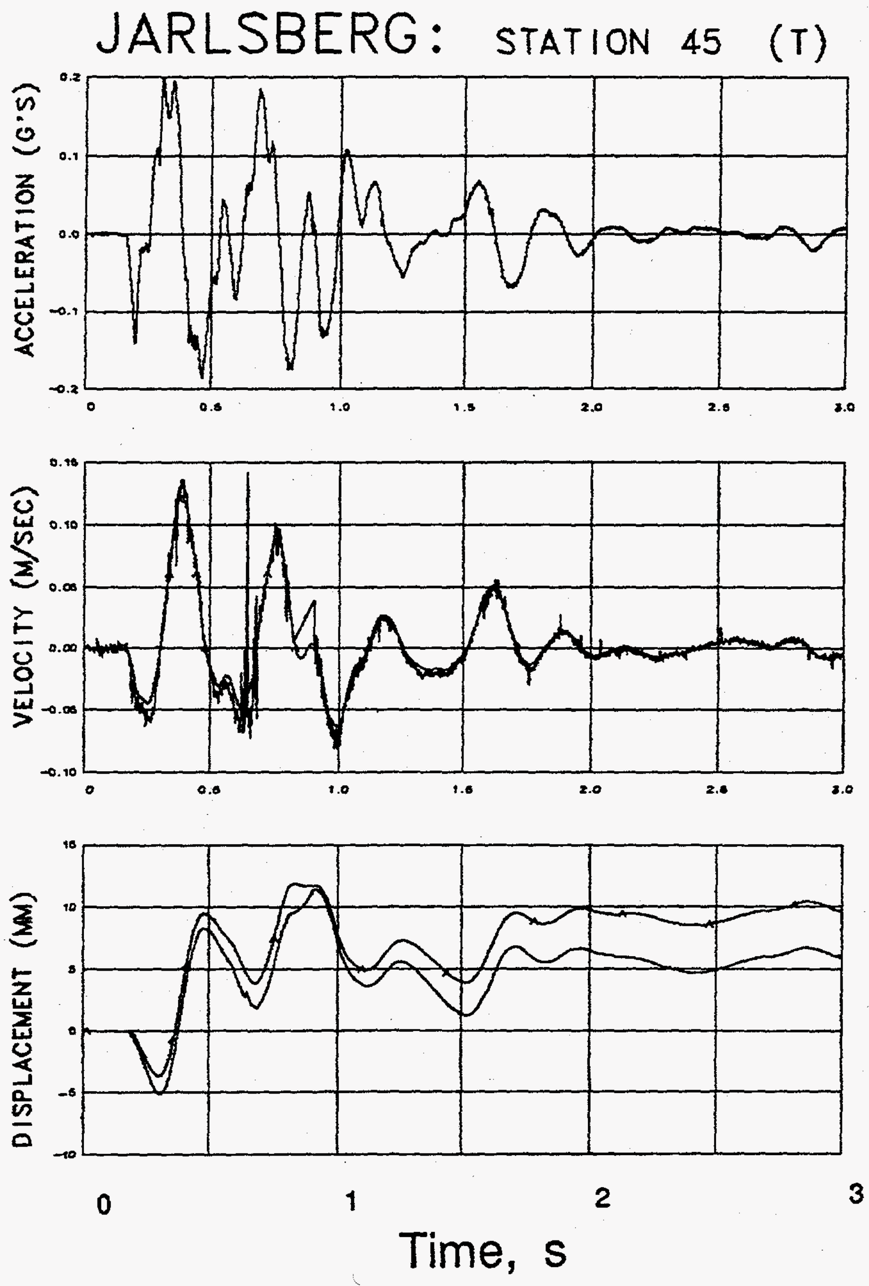


Figure 5.9 Explosion–induced transverse–horizontal motion at a depth of 251 m in hole Ue10aa (station 45). Traces annotated with "A" were derived from the accelerometer.

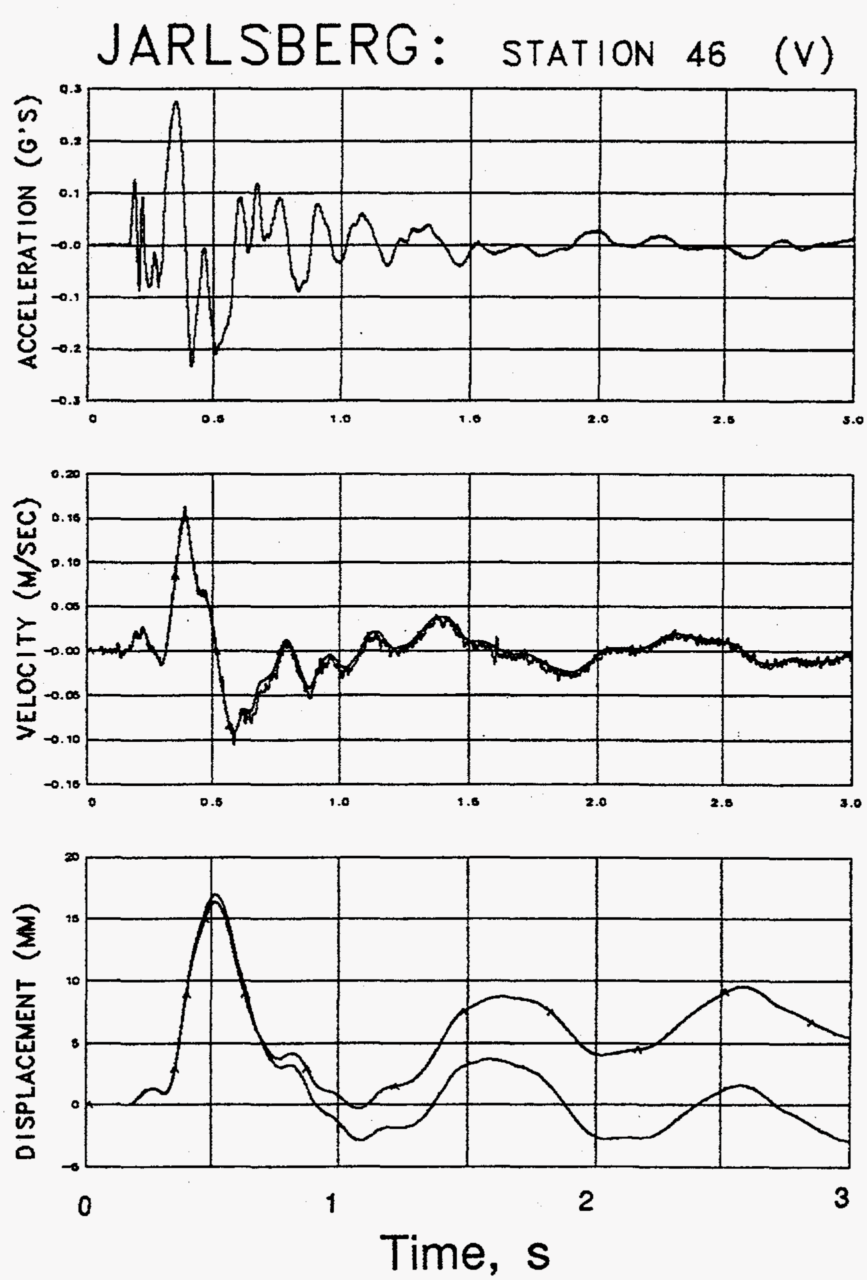


Figure 5.10 Explosion–induced vertical motion at a depth of 198m in hole Ue10aa (station 46). Traces annotated with "A" were derived from the accelerometer.

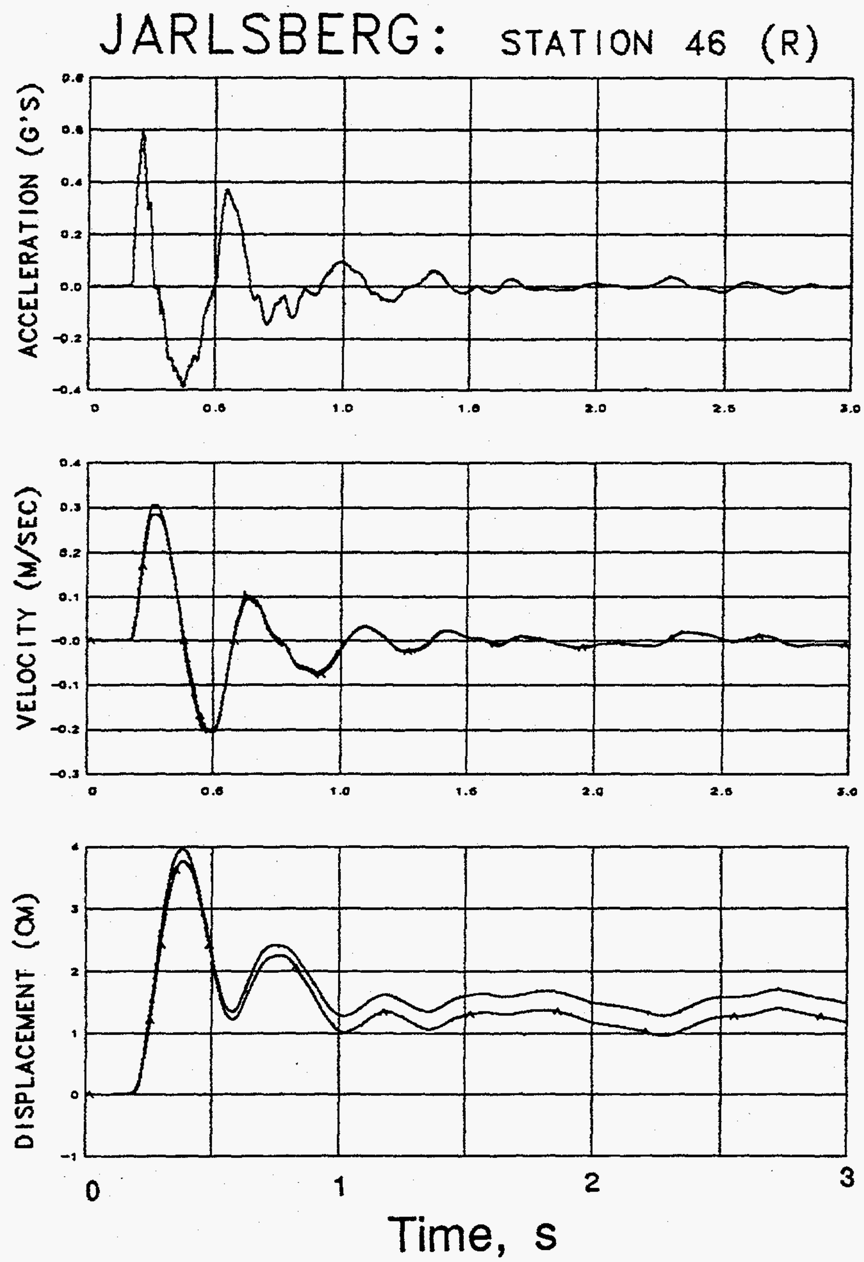


Figure 5.11 Explosion–induced radial–horizontal motion at a depth of 198 m in hole Ue10aa (station 46). Traces annotated with "A" were derived from the accelerometer.

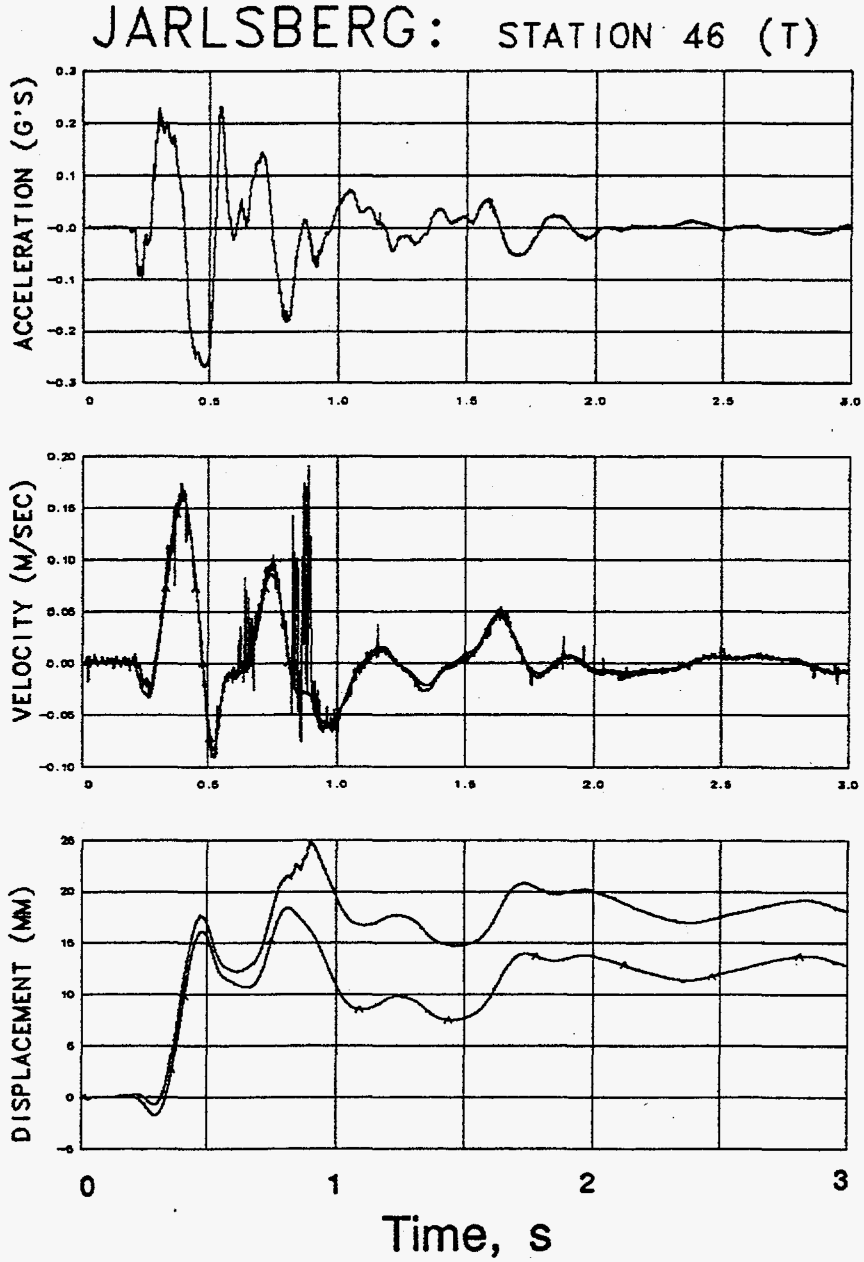


Figure 5.12 Explosion–induced transverse–horizontal motion at a depth of 198 m in hole Ue10aa (station 46). Traces annotated with "A" were derived from the accelerometer.

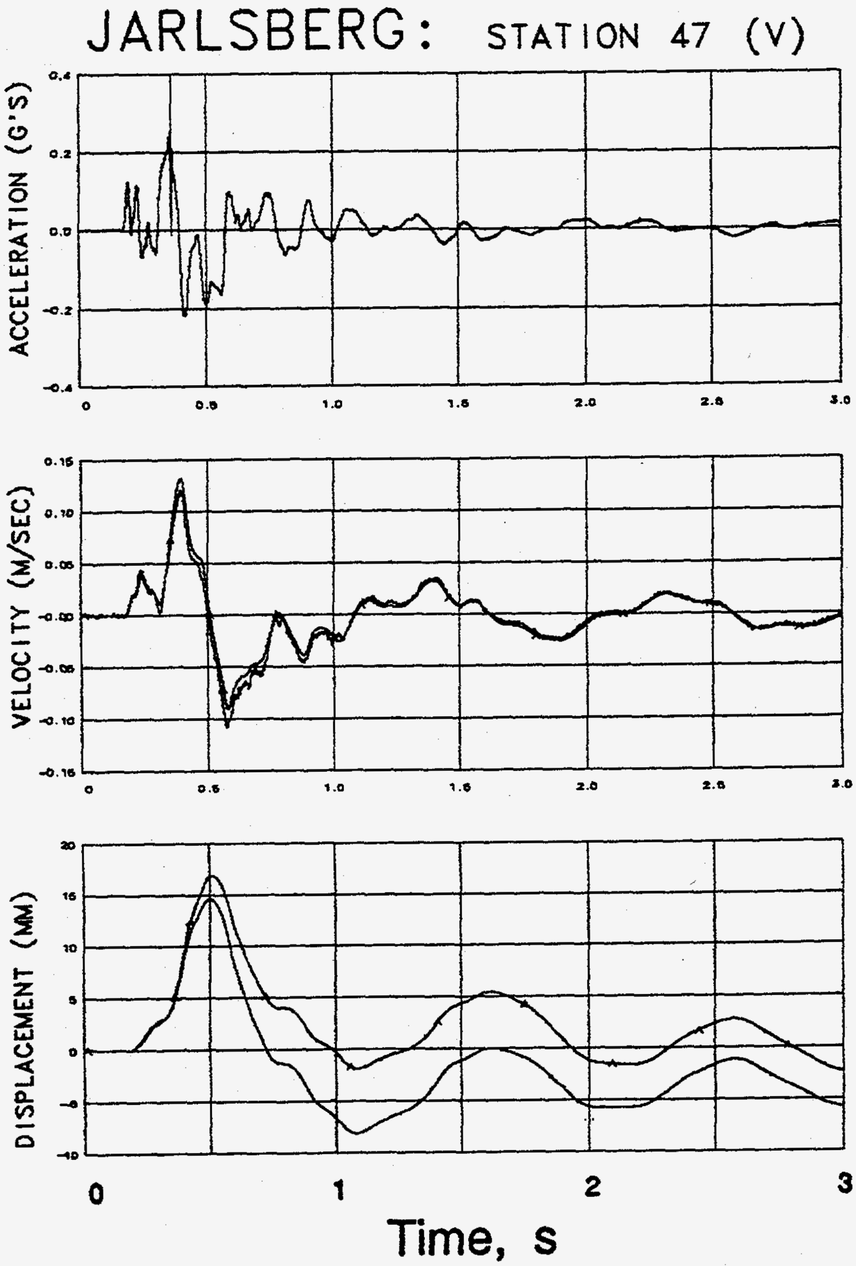


Figure 5.13 Explosion–induced vertical motion at a depth of 173 m in hole Ue10aa (station 47). Traces annotated with "A" were derived from the accelerometer.

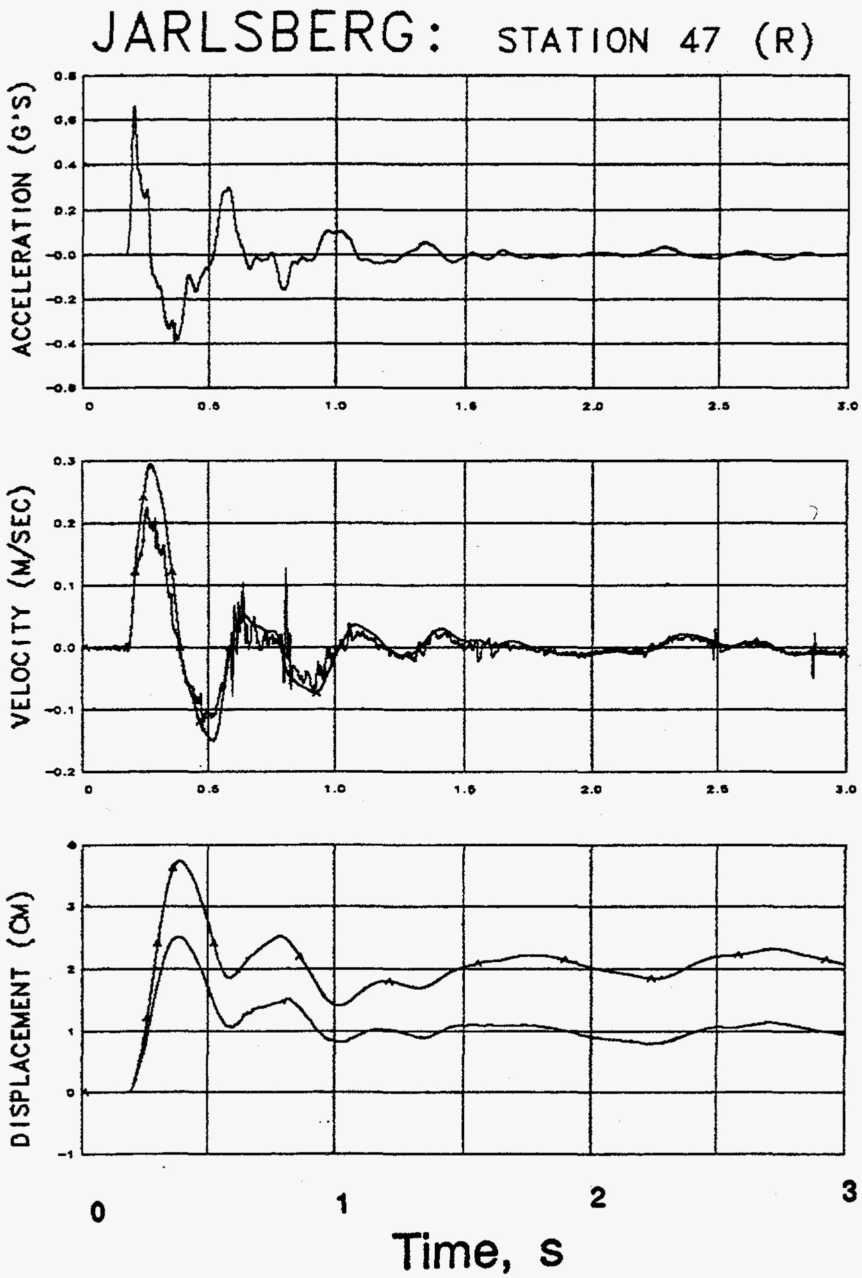


Figure 5.14 Explosion–induced radial–horizontal motion at a depth of 173 m in hole Ue10aa (station 47). Traces annotated with "A" were derived from the accelerometer.

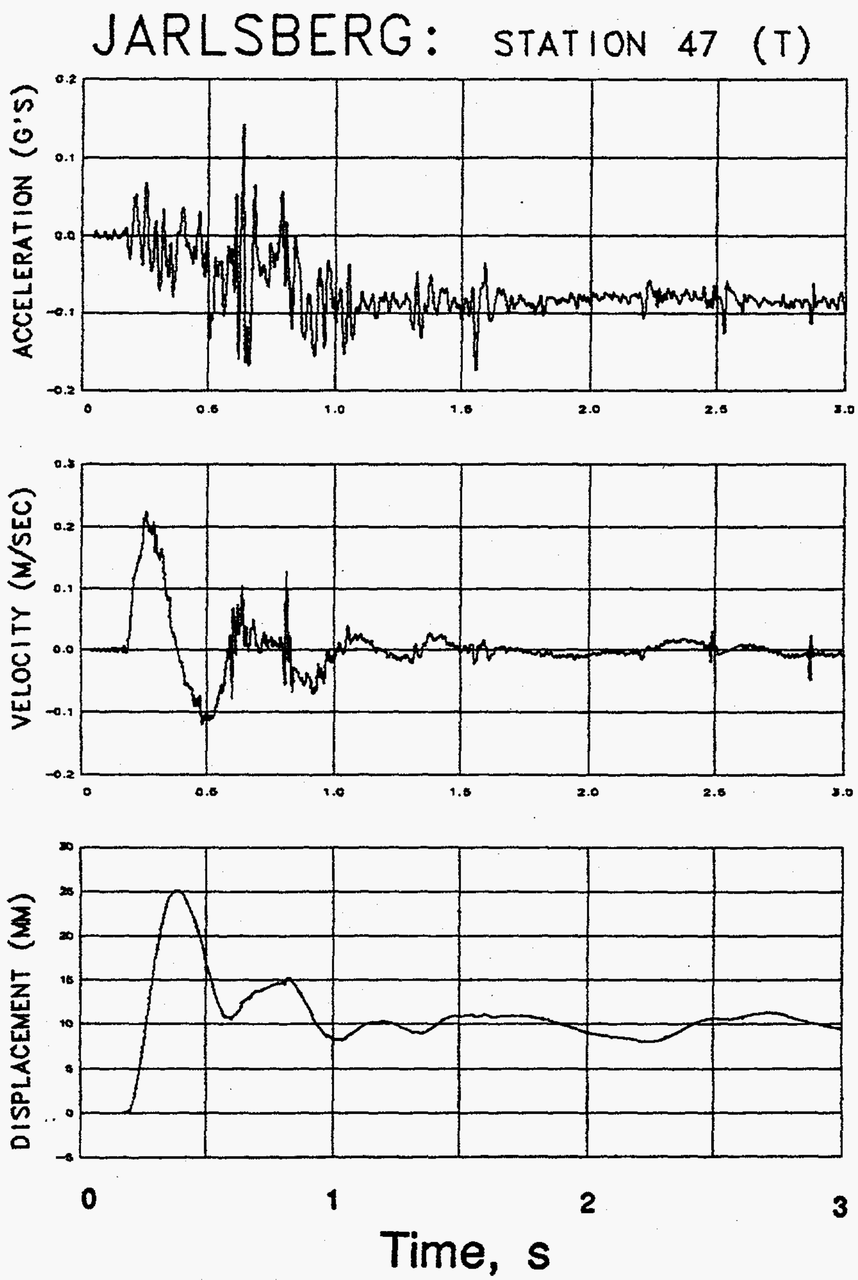


Figure 5.15 Explosion-induced transverse-horizontal motion at a depth of 173 m in hole Ue10aa (station 47). Traces annotated with "A" were derived from the accelerometer.

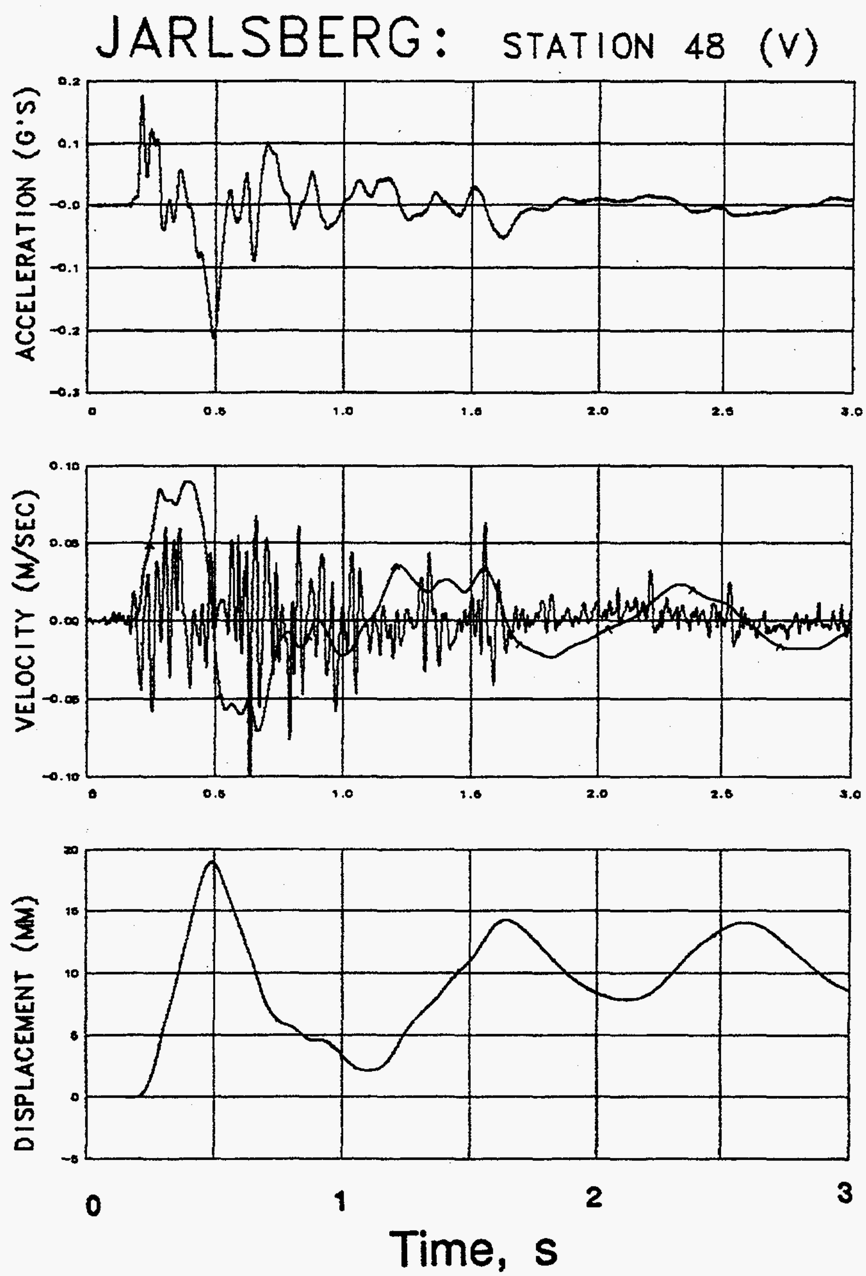


Figure 5.16 Explosion–induced vertical motion at a depth of 113 m in hole Ue10aa (station 48). Traces annotated with "A" were derived from the accelerometer.

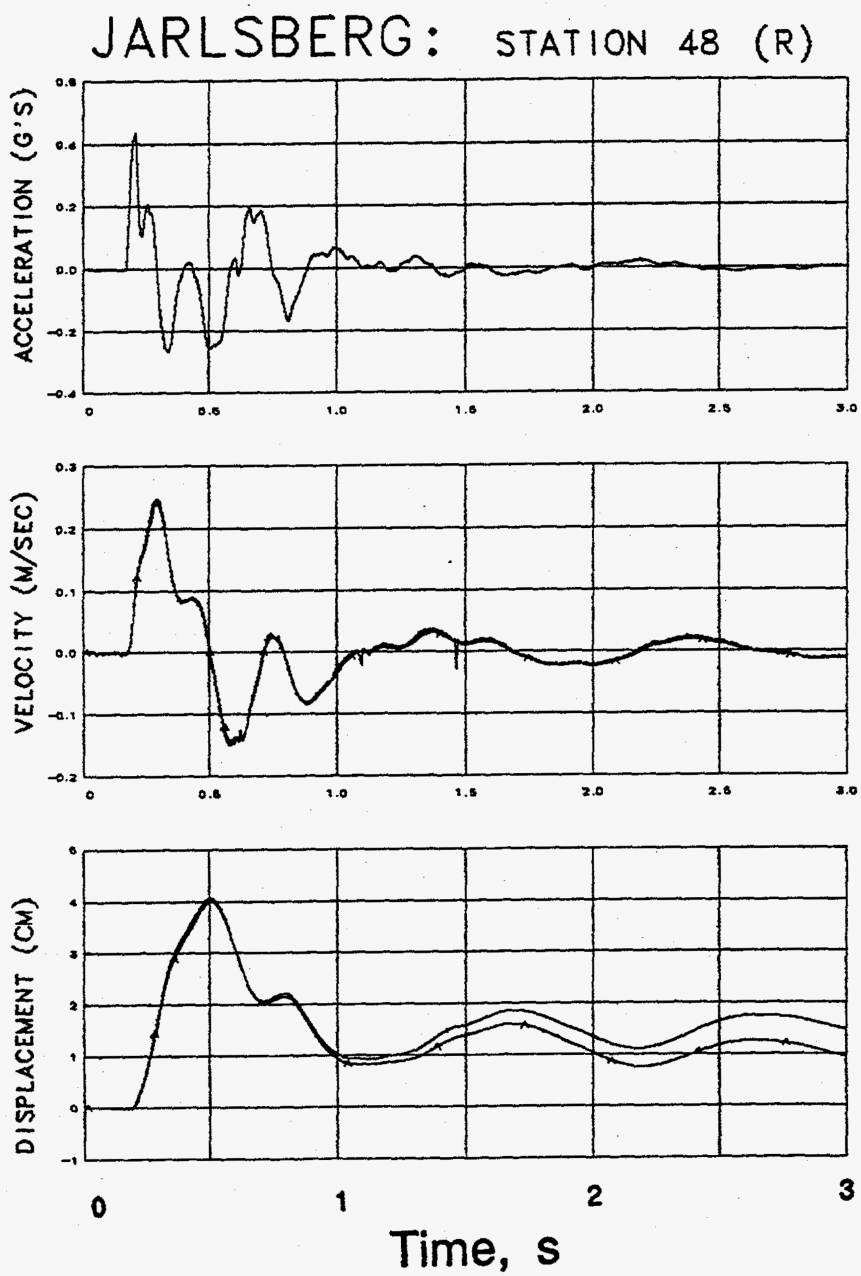


Figure 5.17 Explosion–induced radial–horizontal motion at a depth of 113 m in hole Ue10aa (station 48). Traces annotated with "A" were derived from the accelerometer.

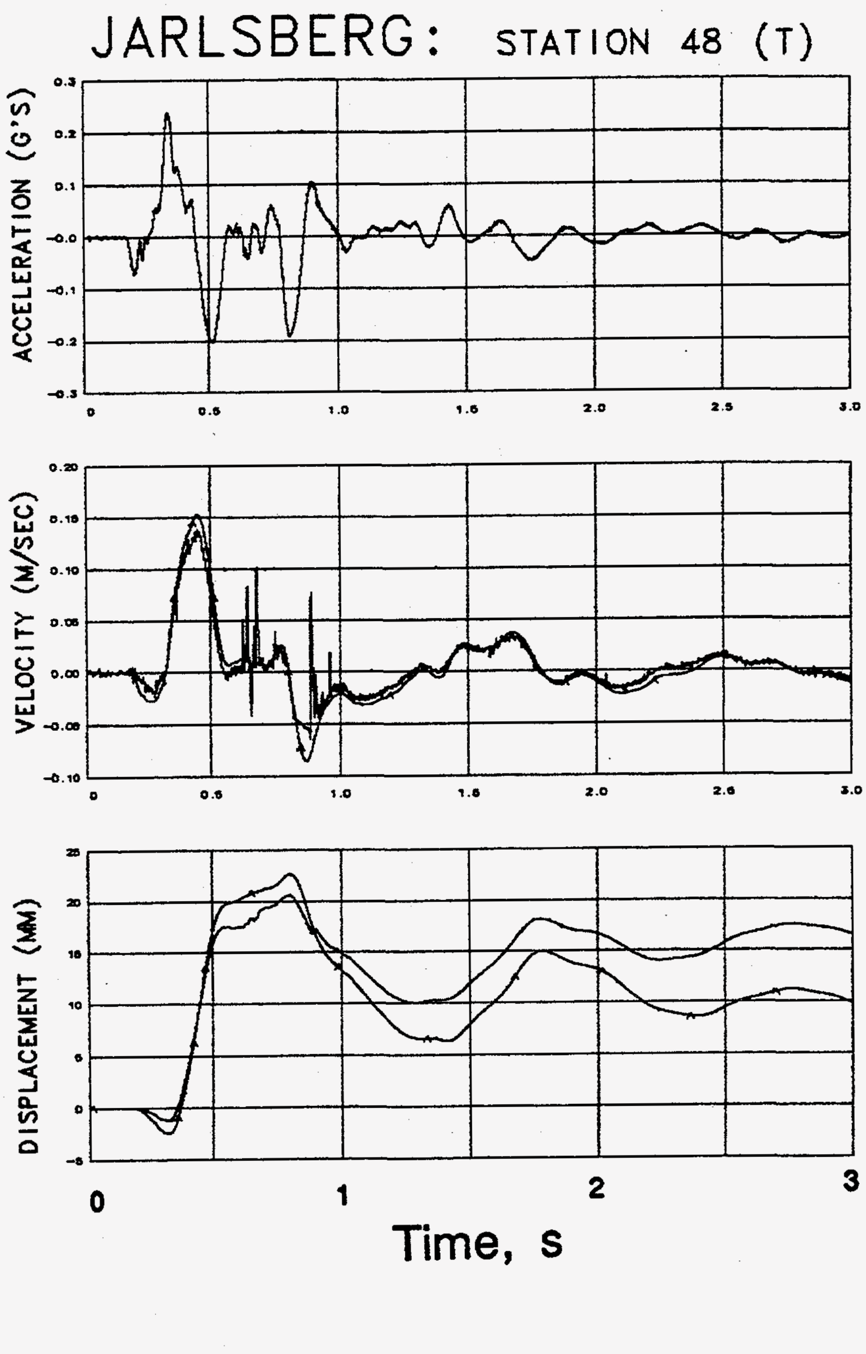


Figure 5.18 Explosion–induced transverse–horizontal motion at a depth of 113 m in hole Ue10aa (station 48). Traces annotated with "A" were derived from the accelerometer.

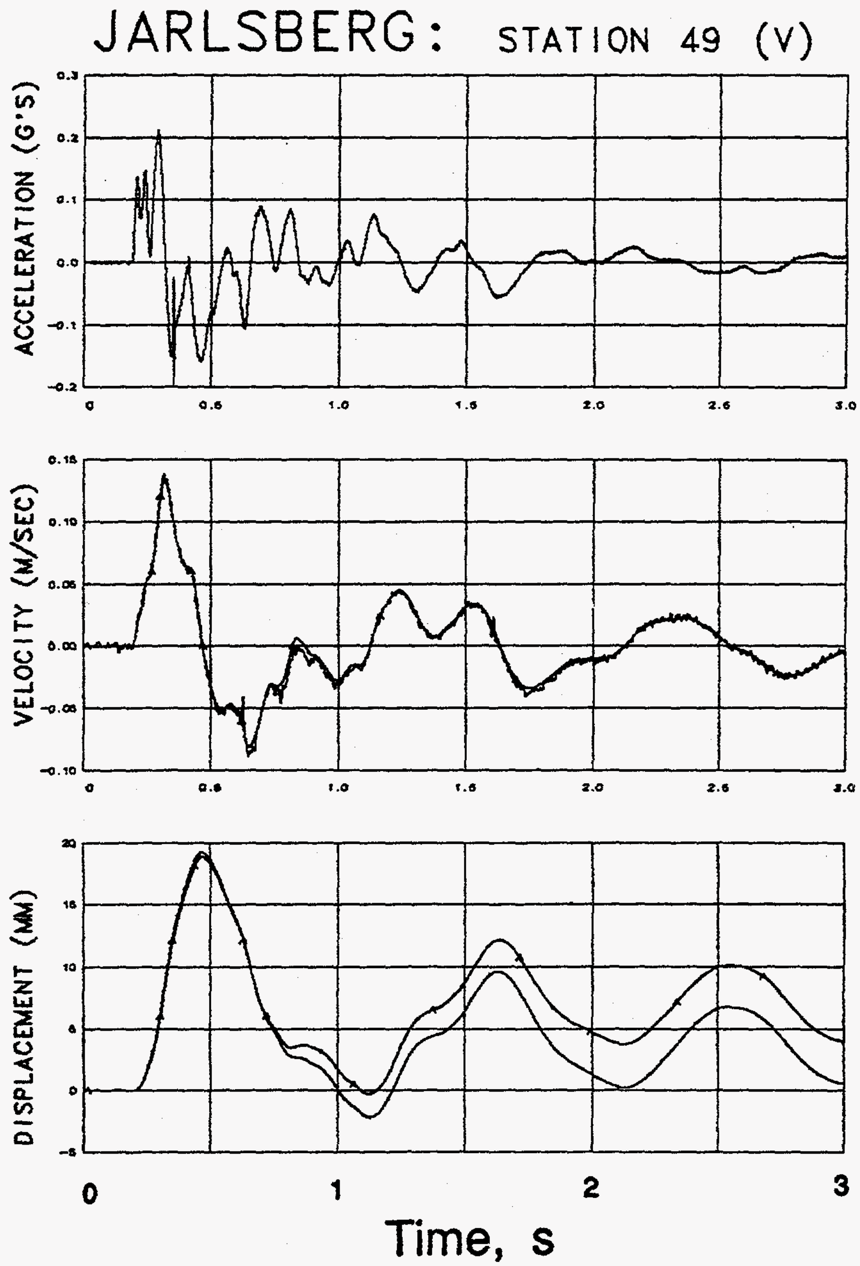


Figure 5.19 Explosion–induced vertical motion at a depth of 56m in hole Ue10aa (station 49). Traces annotated with "A" were derived from the accelerometer.

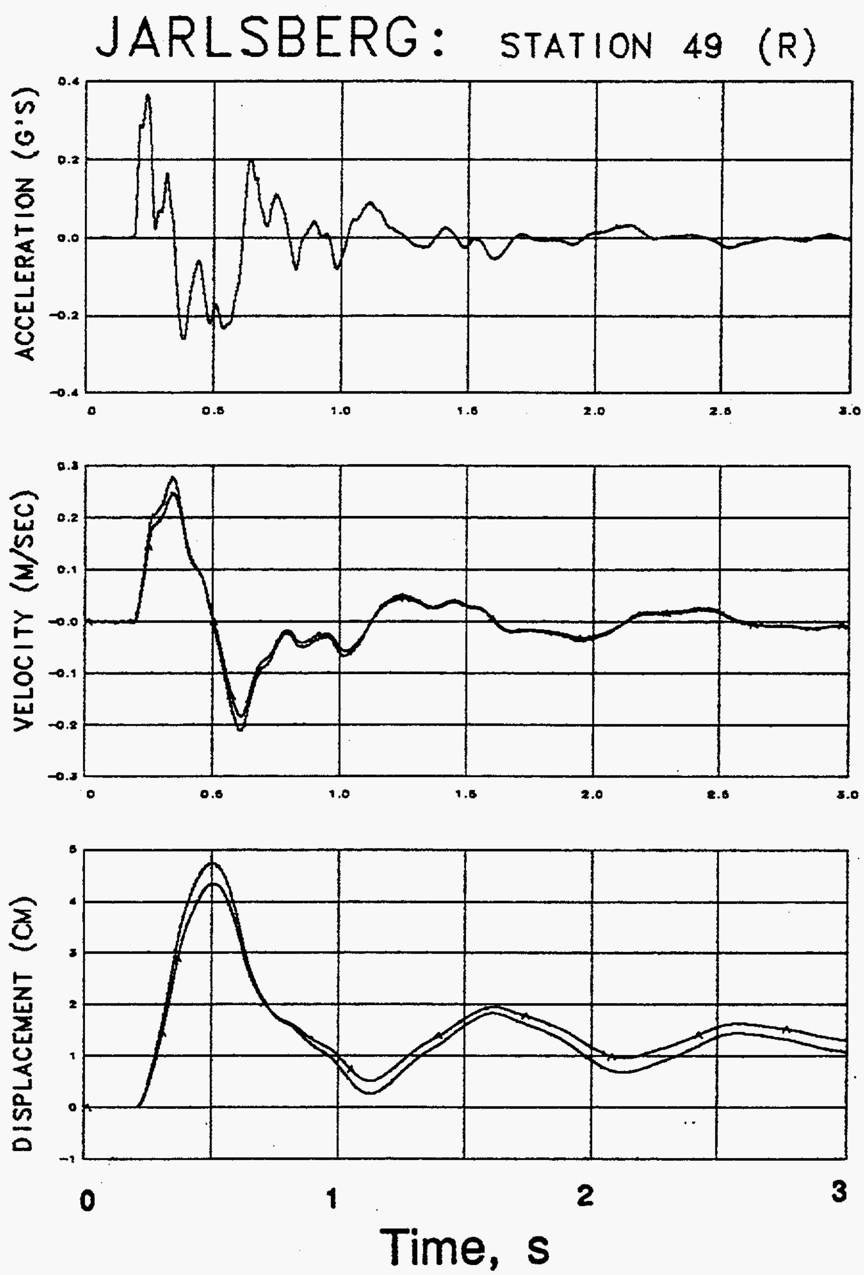


Figure 5.20 Explosion–induced radial–horizontal motion at a depth of 56 m in hole Ue10aa (station 49). Traces annotated with "A" were derived from the accelerometer.

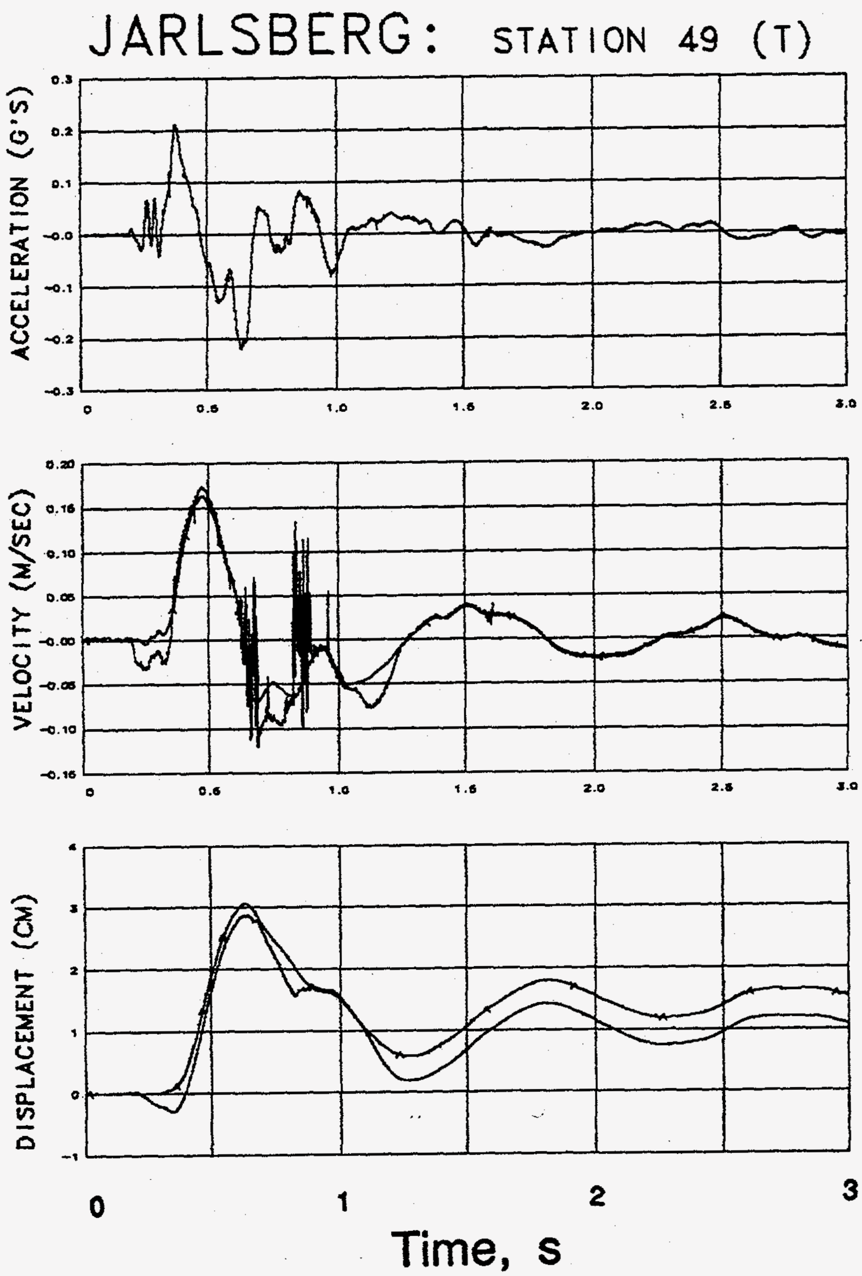


Figure 5.21 Explosion–induced transverse–horizontal motion at a depth of 56 m in hole Ue10aa (station 49). Traces annotated with "A" were derived from the accelerometer.

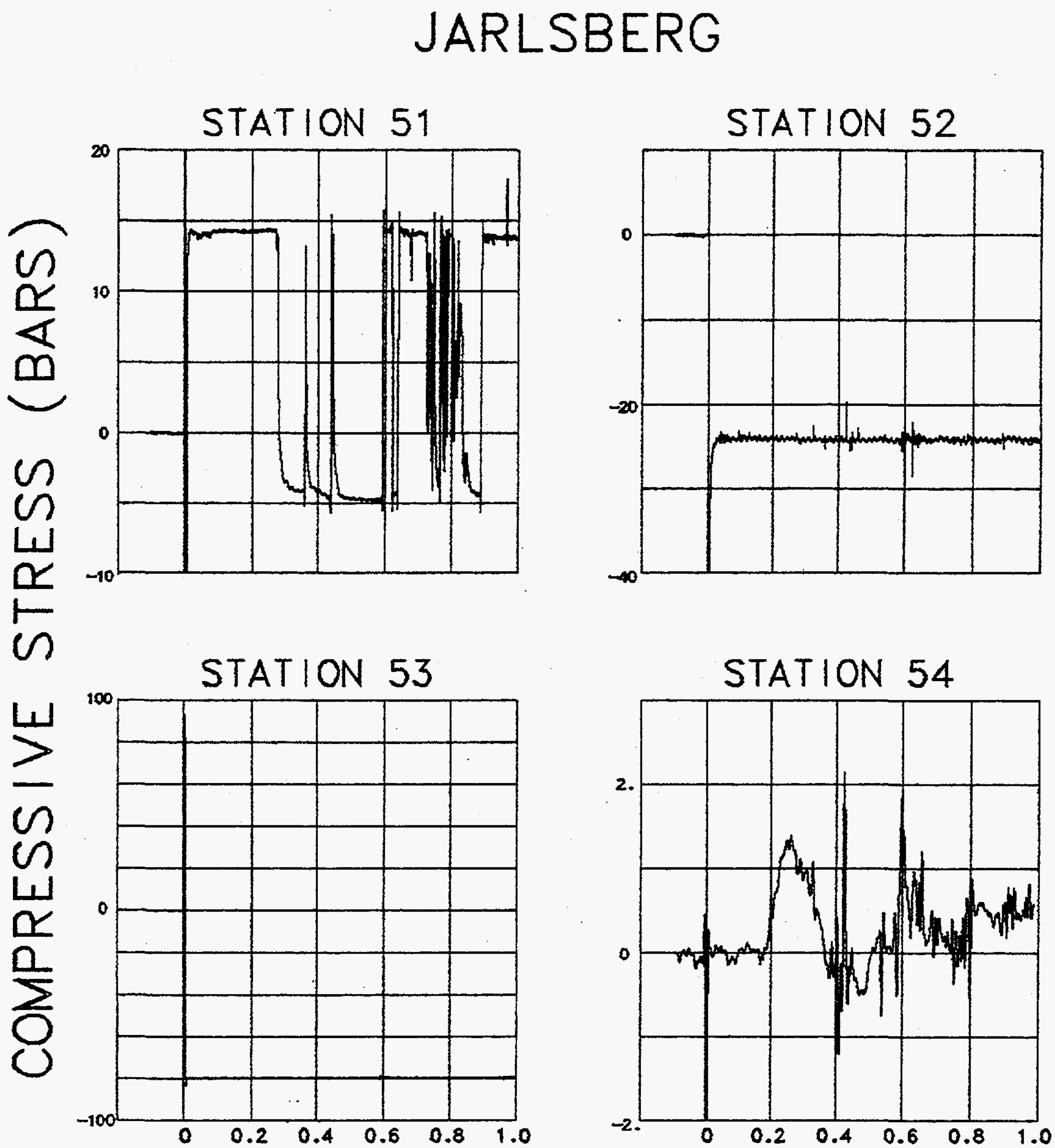


Figure 5.22. Mean stress (pressure) measured in hole Ue10aa. It is suggested that only station 54 reported valid information. Stations 55 and 56 were inoperative pre–shot and not recorded.

## Table 5.1

## Satellite Hole (free–field) Motion Summary

| Gauge | Slant Range (m) | Arrival Time (ms) | Peak Acceleration (g) | Peak Velocity (m/s) | Peak Displacement (m) | Residual Displacement (mm) |
|---|---|---|---|---|---|---|
| 41av | | 138 | 0.24 | 0.99 | 0.006 | 10 |
| 41uv | (a) | | | | | |
| 41ar | 361.0 | 136 | 0.146 | 0.042 | 0.0075 | 3 |
| 41ur | | | | 0.112 | 0.014 | 2 |
| 41at | (b) | 141 | 0.048 | 0.100 | 0.0032 | -8 |
| 41ut | | | | -0.056 | -0.0062 | 1 |
| 44av | | 156 | -0.28 | -0.110 | -0.0083 | -9 |
| 44uv | | | | -0.110 | -0.0083 | 0 |
| 44ar | 327.4 | 159 | 0.44 | 0.187 | 0.0264 | 17 |
| 44ur | | | | 0.196 | 0.0277 | 14 |
| 44at | | 158 | -0.103 | -0.037 | -0.0022 | 4 |
| 44ut | | | | -0.037 | -0.0022 | 7 |
| 45av | | 156 | -0.27 | -0.092 | -0.0054 | -7 |
| 45uv | | | | -0.096 | -0.0052 | 2 |
| 45ar | 314.7 | 152 | 0.59 | 0.240 | 0.0367 | 18 |
| 45ur | | | | -0.250 | 0.0375 | 15 |
| 45at | | 154 | -0.14 | -0.045 | -0.0037 | 8 |
| 45ut | | | | -0.058 | -0.0050 | 6 |
| 46av | | 162 | 0.125 | 0.021 | 0.0164 | 7 |
| 46uv | | | | 0.022 | 0.0172 | 3 |
| 46ar | 310.5 | 166 | 0.600 | 0.280 | 0.0375 | 12 |
| 46ur | | | | 0.310 | 0.0396 | 15 |
| 46at | | 166 | -0.095 | -0.033 | -0.0018 | 12 |
| 46ut | | | | -0.025 | -0.0010 | 17 |
| 47av | | 168 | 0.123 | 0.038 | 0.0013 | 0 |
| 47uv | | | | 0.044 | 0.00145 | -3 |
| 47ar | 312.2 | 168 | 0.660 | 0.294 | 0.0372 | 20 |
| 47ur | | | | 0.320 | 0.0395 | 15 |
| 47at | (a) | | | | | |
| 47ut | | 180 | | -0.050 | -0.0032 | 8 |
| 48av | | 168 | 0.175 | 0.084 | 0.0189 | 10 |
| 48uv | (a) | | | | | |
| 48ar | 328.0 | 166 | 0.430 | 0.244 | 0.0400 | 10 |
| 48ur | | | | 0.248 | 0.0405 | 15 |
| 48at | | 166 | -0.071 | -0.028 | -0.0025 | 7 |
| 48ut | | | | -0.022 | -0.0011 | 17(c) |
| 49av | | 185 | 0.135 | 0.133 | 0.0188 | 6 |
| 49uv | | | | 0.137 | 0.0187 | 5 |
| 49ar | 342.8 | 185 | 0.365 | 0.248 | 0.0433 | 13 |
| 49ur | | | | 0.277 | 0.0470 | 11 |
| 49at | | 184 | -0.033 | 0.160 | 0.0305 | 15 |
| 49ut | | | | (c) | | |

(a) Malfunction.
(b) These data are highly questionable.
(c) Data invalid: noise influences magnitude

## Table 5.2

## Satellite Hole Accelerometer Characteristics†

| Gauge | Natural Frequency (Hz) | Damping Ratio | System Range (g) |
|---|---|---|---|
| 41av | 182 | 0.70 | 1.6 |
| 41ar | 138 | 0.65 | 1.6 |
| 41at | 175 | 0.70 | 2.0 |
| 44av | 180 | 0.70 | 2.0 |
| 44ar | 122 | 0.75 | 2.0 |
| 44at | 158 | 0.85 | 2.0 |
| 45av | 170 | 0.65 | 2.0 |
| 45ar | 117 | 0.65 | 2.0 |
| 45at | 132 | 0.65 | 2.0 |
| 46av | 175 | 0.70 | 2.0 |
| 46ar | 170 | 0.65 | 2.0 |
| 46at | 145 | 0.70 | 2.0 |
| 47av | 175 | 0.60 | 2.0 |
| 47ar | 175 | 0.75 | 2.0 |
| 47at | 145 | 0.65 | 2.0 |
| 48av | 184 | 0.65 | 2.0 |
| 48ar | 169 | 0.70 | 2.0 |
| 48at | 145 | 0.75 | 2.0 |
| 49av | 170 | 0.65 | 2.0 |
| 49ar | 120 | 0.65 | 2.0 |
| 49at | 152 | 0.60 | 2.0 |

† All accelerometers are variable reluctance devices

## Table 5.3

## Satellite Hole Velocimeter Characteristics

| Gauge | Natural Frequency (Hz) | Time to 0.5 Amplitude (s) | Calibration Temperature ($^oC$) | Operate Temperature ($^oC$) | System Range (m/s) |
|---|---|---|---|---|---|
| 41uv | 3.566 | 8.89 | 23.899 | 29.91 | 1.4 |
| 41ur | 3.600 | 9.39 | 24.17 | 29.91 | 1.4 |
| 41ut | 3.594 | 9.38 | 24.07 | 29.91 | 1.4 |
| 44uv | 3.543 | 8.82 | 25.80 | 28.93 | 2.0 |
| 44ur | 3.518 | 9.94 | 22.54 | 28.93 | 2.0 |
| 44ut | 3.556 | 9.17 | 24.08 | 28.93 | 2.0 |
| 45uv | 3.657 | 8.61 | 25.90 | 27.05 | 2.0 |
| 45ur | 3.502 | 9.38 | 24.24 | 27.05 | 2.0 |
| 45ut | 3.384 | 9.28 | 24.55 | 27.05 | 2.0 |
| 46uv | 3.518 | 9.74 | 26.05 | 23.61 | 2.0 |
| 46ur | 3.444 | 9.30 | 24.34 | 23.61 | 2.0 |
| 46ut | 3.624 | 9.50 | 22.73 | 23.61 | 2.0 |
| 47uv | 3.551 | 9.22 | 25.46 | 22.89 | 2.0 |
| 47ur | 3.685 | 9.36 | 22.82 | 22.89 | 2.0 |
| 47ut | 3.577 | 9.20 | 23.06 | 22.89 | 2.0 |
| 48uv | 3.640 | 8.38 | 25.63 | 18.83 | 2.0 |
| 48ur | 3.452 | 8.82 | 24.46 | 18.83 | 2.0 |
| 48ut | 3.362 | 9.76 | 22.77 | 18.83 | 2.0 |
| 49uv | 3.396 | 10.32 | 25.72 | 17.73 | 2.0 |
| 49ur | 3.512 | 9.21 | 22.39 | 17.73 | 2.0 |
| 49ut | 3.464 | 9.27 | 22.40 | 17.73 | 2.0 |

## References

(1) J L. Wagoner and S. R. Clark, "U10ca, 210 m, Preliminary Site Characteristics Summary", CP 83–28, Lawrence Livermore National Laboratory, CA, April 15, 1983.

(2) William G. Webb, "Special Measurements Physics/Instrumentation Package for JARLSBERG/FIRESTORM, U10ca, Ue10aa, Revision A, Final", EG&G, Energy Measurements, Las Vegas Operations, SM:83E–108–20,12 October, 1983.

(3) Alfred E. Burer, "Containment Report for U10ca", Holmes & Narver, Inc., NTS:A2:83–33, August 26, 1983.

(4) William G. Webb, "Special Measurements Final Engineering Report, JARLSBERG, U10ca, Ue10aa", EG&G, Energy Measurements, Las Vegas Operations, SM:83E–108–19, 12 October, 1983.

Distribution:

**LLNL**

| | |
|---|---|
| TID (11) | L-053 |
| Test Program Library | L-045 |
| Containment Vault | L-221 |
| Burkhard, N. | L-221 |
| Cooper, W. | L-049 |
| Denny, M. | L-205 |
| Dong, R. | L-140 |
| Goldwire, H. | L-221 |
| Heinle, R. (5) | L-221 |
| Mara, G. | L-049 |
| Moran, M.T. | L-777 |
| Moss, W. | L-200 |
| Olsen, C. | L-221 |
| Patton, H, | L-205 |
| Pawloski, G. | L-221 |
| Rambo, J. | L-200 |
| Roland, K. | L-221 |
| Roth, B. | L-049 |
| Valk, T. | L-154 |
| Younker, L. | L-203 |

**LANL**

| | |
|---|---|
| App, F. | F-659 |
| Brunish, W. | F-659 |
| Kunkle, T. | F-665 |
| Trent, B. | F-664 |

**Sandia**

| | |
|---|---|
| Chabai, A. | MS-1159 |
| Smith, Carl W. | MS-1159 |

**EG&G/AVO**

| | |
|---|---|
| Brown, T. | A-5 |
| Gilmore, L. | A-1 |
| Hatch, M. | A-5 |
| Still, G. | A-5 |
| Stubbs, T. | A-5 |

**EG&G/NVO**

| | |
|---|---|
| Bellow, B. | N 13-20 |
| Davies, L. | N 13-20 |
| Moeller, A. | N 13-20 |
| Robinson, R. | N 13-20 |
| Webb, W. | N 13-20 |

**DNA**

Ristvet, B.

**S-Cubed**

Peterson, E.

**Eastman Cherrington Environment**
1640 Old Pecos Trail, Suite H
Santa Fe, NM 87504

Keller, C.